



Pigot, A. L., Sheard, C., Miller, E. T., Bregman, T. P., Freeman, B. G., Roll, U., Seddon, N., Trisos, C. H., Weeks, B. C., & Tobias, J. A. (2020). Macroevolutionary convergence connects morphological form to ecological function in birds. *Nature Ecology and Evolution*, 4, 230-239 (2020). <https://doi.org/10.1038/s41559-019-1070-4>

Peer reviewed version

Link to published version (if available):  
[10.1038/s41559-019-1070-4](https://doi.org/10.1038/s41559-019-1070-4)

[Link to publication record in Explore Bristol Research](#)  
PDF-document

This is the author accepted manuscript (AAM). The final published version (version of record) is available online via Nature Research at <https://doi.org/10.1038/s41559-019-1070-4> . Please refer to any applicable terms of use of the publisher.

## University of Bristol - Explore Bristol Research

### General rights

This document is made available in accordance with publisher policies. Please cite only the published version using the reference above. Full terms of use are available:  
<http://www.bristol.ac.uk/red/research-policy/pure/user-guides/ebr-terms/>

# Macroevolutionary convergence connects morphological form to ecological function in birds

**Authors:** Alex L. Pigot<sup>1,2†\*</sup>, Catherine Sheard<sup>3,2†</sup>, Eliot T. Miller<sup>4,5</sup>, Tom P. Bregman<sup>6,2</sup>, Benjamin G. Freeman<sup>7</sup>, Uri Roll<sup>8,2</sup>, Nathalie Seddon<sup>2</sup>, Brian C. Weeks<sup>9,10</sup>, Joseph A. Tobias<sup>11,2\*</sup>

## Affiliations:

<sup>1</sup>Centre for Biodiversity and Environment Research, Department of Genetics, Evolution and Environment, University College London, Gower Street, London, WC1E 6BT, UK.

<sup>2</sup>Department of Zoology, University of Oxford, South Parks Road, Oxford, OX1 3PS, UK.

<sup>3</sup>School of Biology, University of St Andrews, Fife, KY16 9TJ, UK.

<sup>4</sup>Cornell Lab of Ornithology, 159 Sapsucker Woods Rd., Ithaca, NY 14850, USA.

<sup>5</sup>Department of Biological Sciences, University of Idaho, Moscow, Idaho 83844, USA.

<sup>6</sup>Future-Fit Foundation, 1 Primrose Street, Spitalfields, London, EC2A 2EX, UK.

<sup>7</sup>Biodiversity Research Centre, University of British Columbia, 6270 University Blvd., Vancouver BC, V6T 1Z4, Canada.

<sup>8</sup>Mitrani Department of Desert Ecology, Jacob Balaustein Institutes for Desert Research, Ben-Gurion University of the Negev, Midreshet Ben-Gurion 8499000, Israel.

<sup>9</sup>School for Environment and Sustainability, University of Michigan, Ann Arbor, MI 48109, USA.

<sup>10</sup>Department of Ornithology, American Museum of Natural History, 79<sup>th</sup> Street at Central Park West, New York, NY 10024, USA.

<sup>11</sup>Department of Life Sciences, Imperial College London, Silwood Park, Buckhurst Road, Ascot SL5 7PY, UK.

†Equal contribution

\*Correspondence to: [a.pigot@ucl.ac.uk](mailto:a.pigot@ucl.ac.uk); [j.tobias@imperial.ac.uk](mailto:j.tobias@imperial.ac.uk)

Word count: Abstract (154), Main text (3,132), Methods (3,654), Captions for 6 figures (581)

References: Main text (52), Total (75)

**Animals have diversified into a bewildering variety of morphological forms exploiting a complex configuration of trophic niches. Their morphological diversity is widely used as an index of ecosystem function, but the extent to which animal traits predict trophic niches and associated ecological processes is unclear. Here we use measurements of nine key morphological traits for >99% bird species to show that avian trophic diversity is described by a trait space with four dimensions. The position of species within this space maps with 70-85% accuracy onto major niche axes, including trophic level, dietary resource type and finer-scale variation in foraging behaviour. Phylogenetic analyses reveal that these form-function associations reflect convergence towards predictable trait combinations, indicating that morphological variation is organised into a limited set of dimensions by evolutionary adaptation. Our results establish the minimum dimensionality required for avian functional traits to predict subtle variation in trophic niches, and provide a global framework for exploring the origin, function and conservation of bird diversity.**

Plants and animals have complementary functions in the biosphere, with plants mainly contributing as autotrophic producers and animals occupying multiple higher trophic levels as primary, secondary and tertiary consumers<sup>1-4</sup>. Restriction of most plant species to a single trophic level at the foundation of food webs theoretically limits the scope for niche variation, perhaps explaining why their vast trait diversity is predominantly constrained to a simple plane with two dimensions<sup>5</sup>. In contrast, the ecological trait space of heterotrophic consumers is potentially more complex and multidimensional<sup>6-9</sup>, particularly if distinct sets of morphological traits are consistently associated with different trophic levels and dietary types—including herbivores, pollinators and predators<sup>10</sup>. This concept of a predictable link between animal form and function has existed since Aristotle<sup>11</sup> and now underpins numerous trait-based research programmes<sup>12</sup>, from resolving the evolutionary origins of biodiversity<sup>13,14</sup> to quantifying ecosystem function<sup>15,16</sup> and predicting responses to environmental change<sup>17,18</sup>. However, the assumption that ecological niche space and associated ecosystem functions can be adequately quantified using a limited set of phenotypic traits remains controversial<sup>19,20</sup>.

At one extreme of complexity, species and their traits may be embedded within an abstract multidimensional niche space, the '*n*-dimensional hypervolume' of G. E. Hutchinson<sup>21</sup>. By assuming an almost limitless number of ecological dimensions, this model provides a compelling explanation for the diversity of species and phenotypes found in nature<sup>13,14,21</sup>. At the other extreme, the mapping of traits onto niche space may be simplified to a single dimension<sup>22-24</sup> by functional trade-offs<sup>25</sup> or pervasive convergent evolution<sup>26,27</sup>. Whether form-function relationships are either unfathomably complex or unexpectedly simple has major implications for the usefulness of trait-based approaches to quantifying and conserving biodiversity<sup>16,28,29</sup>.

In a high-dimensional Hutchinsonian niche space, pinpointing the functional role of a species would require numerous axes of phenotypic variation<sup>30</sup>, potentially confounding efforts to understand niches based on standardised trait datasets<sup>12,15,17,18</sup>. Conversely, if most of the diversity in functional traits can be collapsed along one or two fundamental dimensions, then this may not provide sufficient traction for traits to be informative about multiple ecological functions, particularly in multitrophic systems<sup>19,28</sup>. Some ecomorphological analyses have found evidence that the dimensionality of animal hypervolumes may lie somewhere between these extremes<sup>30-32</sup>, raising hope that trait combinations could be partitioned into a relatively simplistic niche classification system—analogueous to the periodic table of elements<sup>27</sup>. Yet, previous studies have focused on restricted spatial and taxonomic scales, producing contradictory results and no clear consensus about the structure or generality of form-function relationships in animals<sup>31-36</sup>.

Here we present the first comprehensive assessment of phenotypic trait diversity for extant birds (Aves), the largest class of tetrapod vertebrates. For over a century, birds have played a central role in the development of niche concepts and ecomorphology<sup>31,37-39</sup>, and now provide the richest template for exploring the function and evolution of morphological traits in the context of species-level ecological<sup>40</sup> and phylogenetic datasets<sup>41</sup>. We measured eight phenotypic traits with well-established connections to locomotion, trophic ecology, and the associated niche structure of ecological communities<sup>31,32,39,42</sup> (Extended Data Fig. 1, see Methods). In particular, the beak is the primary apparatus used by birds to capture and process food<sup>39,43</sup>, while morphological differences in wings, tails and legs are related to locomotion, providing insight into the way birds move through their environment and forage for resources<sup>31</sup>. With the addition of body mass, our dataset contains full sets of nine traits for 9,963

species, representing >99% of extant bird diversity and all 233 avian families (Extended Data Table 1), thereby summarizing whole-organism trait combinations in unprecedented detail for a major radiation of organisms distributed worldwide across marine and terrestrial biospheres. We use a range of analyses to explore the structure of this trait diversity and its connection to ecological function.

### **The multiple dimensions of avian trait space**

Across birds, body mass varies by a factor of 50,000 (Fig. 1a) and the position of species along this single axis has important associations with metabolism and life history<sup>44</sup>. To go beyond this basic variation among organisms, we can visualise avian trait diversity by projecting species into a multivariate space (hereafter, morphospace) derived from principal component (PC) scores (see Methods). These projections can be restricted to the beak (Fig. 1b, Extended Data Table 2) or expanded to encompass all traits (Fig. 1c, Extended Data Table 3), in both cases revealing enormous variation in size (PC1) and shape (PC2-PC3).

Unlike the bimodal distribution of plant forms<sup>5</sup>, variation in bird traits is centred on a single dense core around which species with extreme morphologies are scattered at the periphery of morphospace (Fig. 1b-c, Extended Data Figs. 3,4). The structure of these three-dimensional projections highlights the diversity of ways that birds have explored different trait combinations. For instance, the second dimension of total trait variation (PC2; 6% trait variance) describes the spectrum from small to large beaks, while the third dimension (PC3; 4% of trait variance) separates species with short tails and pointed beaks (e.g. kiwis) from those with long tails and stubby beaks (e.g. frogmouths) (Extended Data Fig. 3). Compared to the primary axis of body size (PC1), along which most (83%) phenotypic variation is aligned, these and the remaining

dimensions of avian morphospace constitute only a fraction of total phenotypic variation (17%). However, the key question is whether the position of species in this high-dimensional morphospace provides deeper insight into their ecological function.

### **The mapping of form to function**

To understand how morphology relates to ecological function, we classified species into different types of primary consumers (aquatic and terrestrial herbivores, nectarivores, frugivores, granivores), secondary and tertiary consumers (aquatic carnivores, terrestrial invertivores, terrestrial vertivores), and scavengers (Extended Data Fig. 5a, see Methods). Most avian species are largely specialized on a single trophic level ( $n = 8,343$  species) and, within this, a single trophic niche ( $n = 8,225$  species). The rest constitute omnivores that exploit multiple trophic levels ( $n = 1,620$  species) or niches (either within or across levels,  $n = 1,738$  species) in relatively equal proportions (see Methods). To test whether the location of species in morphospace predicts their trophic niche, we used a Random Forest (RF) model, a type of machine learning algorithm that applies recursive partitioning (i.e. decision trees) to subdivide morphospace into a set of non-overlapping rectangular hypervolumes within which variation in species niches is minimized (see Methods). We began by assessing whether body mass alone can predict species' trophic niche, then added additional traits to build up a progressively more complete description of avian phenotype.

We found that a model using only body mass (Fig. 2a) achieved only limited accuracy in predicting either trophic niches (29%) or broad trophic levels (38%). Only nectar feeding pollinators—many of which, including hummingbirds (Trochilidae), have evolved miniaturized forms to feed on flowers—were predicted consistently by body mass (Fig. 2b). Thus, although body size accounts for most of the variance in our

phenotypic traits (Extended Data Table 3), it provides a relatively weak explanation of avian trophic niche space at global scales. The predictability of trophic niches more than doubled when including beak size and shape (Fig. 2a,c) and increased further to 78% when we used a nine-dimensional morphospace with a full set of beak and body traits (Fig. 2a,d). Moreover, when we excluded omnivores (see Methods), thereby restricting the analysis to species with the most specialized diets, the predictability of trophic niches and trophic levels exceeded 80% (Fig. 2a). These results were robust to the method used to match traits and ecology, with alternative approaches (e.g. discriminant analysis) indicating a similar rise in predictive accuracy as morphological dimensionality increases (Extended Data Fig. 6, see Methods).

To visualize the striking connection between phenotypic form and trophic function, we mapped the density of each specialist trophic niche onto morphospace ( $n = 8,225$ ). Even when projected onto a two-dimensional plane, here defined by beak size and shape, it is clear that each trophic level, and indeed each trophic niche, occupies a largely distinct region of morphospace (Fig. 3). Specialist invertivores ( $n = 4,788$  species) and frugivores ( $n = 1,030$  species) constitute the bulk of avian species diversity and are diffusely distributed around the centre of morphospace (Fig. 3f-g). Species targeting other resource types possess more extreme combinations of beak size and shape, forming tighter clusters around the periphery (Fig. 3a-e,h-i, Extended Data Fig. 4). These clusters have irregular shapes but generally occupy a single contiguous region of morphospace—a ‘phenotypic fingerprint’—concentrated around a unique central peak of high species density. This relatively simple one-to-one mapping of form to function is not an artefact of projecting niches onto a single two-dimensional plane because even in the full nine-dimensional morphospace each trophic niche can be well described by just one or a few rectangular hypervolumes (see Methods).

The ecological relevance of trait variation may extend far beyond predictions of simplistic trophic niches if morphology captures additional axes of ecological divergence, including subtle gradations of behaviour and microhabitat. The intrinsic subdivision of basic trophic niches into numerous variants is best illustrated in birds by terrestrial invertivores that have evolved a remarkable array of foraging techniques, from catching insects in continuous flight (e.g. swallows) to plucking from vegetation (e.g. antshrikes) or hopping on the ground (e.g. pittas) (Fig. 4, Extended Data Fig. 5b). To assess how morphology relates to these more fine-scale aspects of the niche, we re-ran the RF model after subdividing the nine specialist trophic niches into 30 foraging niches (Fig. 2e-g, Extended Data Table 4, see Methods).

As expected, foraging niches are even less predictable than trophic niches or trophic levels on the basis of body size (Fig. 2a). However, predictability increases substantially when using multiple trait-dimensions, with the location in nine-dimensional morphospace accurately predicting not only the type of resources, but also the specific foraging manoeuvre and substrate used by each species (Fig. 2a, e-g). This result shows that most morphological variation encompassed by each trophic niche (Fig. 3) is not simply redundant<sup>35,36</sup>, with numerous different combinations of traits performing similar ecological roles<sup>8</sup>. Instead, the striking correspondence between avian form and function provides continuous metrics for quantifying multitrophic niches with much greater detail and precision than afforded by coarse ecological categories.

### **The dimensionality of trophic niche space**

To investigate the minimum number of dimensions required to predict avian niches, we applied RF models to morphospaces of varying dimensionality, ranging from one to nine

dimensions, exploring all possible combinations of trait axes ( $n = 511$  combinations). Based on estimates of model predictive accuracy, we then calculated the dimensionality ( $D$ ) of trophic niches using Levene's index (see Methods). According to this index,  $D = 9$  if all trait dimensions contribute equally to predicting trophic niches, with  $D$  decreasing towards 1 as predictive accuracy is driven by progressively fewer trait dimensions. Using this approach, we calculated the overall dimensionality of trophic niche space ( $D_{\text{Total}}$ ) as well as the mean dimensionality across individual trophic niches ( $\bar{D}$ ).

We found that dimensionality varied from the two-dimensional niche of nectarivores to the four-dimensional niche of frugivores, and that niches are on average defined by at least three trait dimensions ( $\bar{D} = 3.5$ ) (Extended Data Fig. 7a). The identity of these dimensions varies across niches reflecting adaptations associated with contrasting modes of life (Extended Data Fig. 8). Taking all trophic niches together, an integrated niche space is minimally described by a four-dimensional morphospace ( $D_{\text{Total}} = 4.4$ ). Decreasing dimensionality from four to one dimension results in an almost linear decline in the ability to predict trophic niches, while increasing dimensionality from four dimensions upwards only results in marginal improvement in niche predictability (Extended Data Fig. 7a). Similar estimates of trophic niche dimensionality were obtained regardless of the method used to match traits and ecology (Extended Data Fig. 10) and whether or not we accounted for the phylogenetic non-independence of species (Extended Data Fig. 7b). These consistent results suggest that trophic niche space is inherently, yet nonetheless moderately, multidimensional. On the one hand, a four-dimensional hypervolume challenges the view<sup>23,24</sup> that animal trophic niches can be collapsed along an axis of body size, or indeed any single trait dimension. On the other hand, the level of

dimensionality seems remarkably limited given the scale of ecomorphological variation encompassed by the entire avian radiation.

It seems plausible that our use of simple linear measurements has led to an underestimate of niche dimensionality and that additional or more sophisticated body shape measurements—such as beak curvature<sup>43</sup>—may reveal further axes of ecological variation. However, the increment in niche-related information is likely to be minor at the scale of our analyses, particularly as simulations suggest that our estimate of dimensionality is robust to the addition of numerous alternative traits (Extended Data Fig. 9, see Methods). Limited dimensionality could also reflect the coarseness of our niche classification, so we re-ran RF models based on niches subdivided into more precise categories relating to foraging behaviours and substrates (Extended data Table 4). We found that more trait dimensions are indeed required to predict this finer-grained classification system ( $\bar{D} = 4.1$ ,  $D_{\text{Total}} = 5.6$ ; Extended Data Fig. 7b), with the trait axes defining trophic niches forming a nested subset of those defining foraging niches (Extended Data Fig. 8, see Methods). However, the increase in niche dimensionality is minor, suggesting a hierarchical structure to niche space whereby the same dimensions are repeatedly partitioned across multiple ecological scales<sup>45</sup>. While these results provide compelling evidence that multitrophic niche space is predictably organized along a limited number of fundamental trait dimensions, they tell us little about how this correspondence between form and function has arisen.

## **The evolution of form-function relationships**

One explanation for the apparent matching between form and function is that closely related species tend to occupy the same niche and have similar traits simply due to shared ancestry<sup>46</sup>. Alternatively, each trophic niche may have evolved multiple times,

with the strong match between form and function arising from repeated phenotypic convergence towards the same adaptive optima<sup>26,47</sup>. The extent to which phylogenetic history or adaptive evolution shape current ecological diversity is unclear. To address this, we compared the strength of the relationship observed between form and trophic function to that expected under an evolutionary null model in which similarity in species traits depends on the time elapsed since lineages diverged as well as variation in the rate of stochastic trait evolution (see Methods). We found that this model can account for a substantial fraction of the match between form and trophic niches (Expected accuracy = 65% [95% CI: 60-70%]) but is insufficient to explain the striking predictability of avian ecological functions (Observed accuracy = 85%, Extended Data Fig. 11). Although each trophic niche is populated by multiple distantly related clades (Extended Data Fig. 12a), these lineages are far more tightly packed in morphospace (Fig. 3) than would be expected based on their evolutionary relatedness (Extended Data Fig. 12b). Thus, while our results highlight the major imprint of phylogenetic history in the structuring of avian trophic diversity, they also suggest that the correspondence between form and function requires an adaptive explanation.

To explore these evolutionary patterns in more detail, we identified 91 pairs of avian families with the most similar traits within each trophic niche (see Methods). We found that some (10%) morphologically matched families are sister clades wherein phenotypic similarity can be explained by shared ancestral traits (Fig. 4a). However, most pairings represent much more ancient divergence events (median divergence time = 55 [Interquartile range: 39-75] million years [Ma] versus 28 [Interquartile range: 21-51] Ma for sister clades), suggesting that trait similarity has resulted from convergent evolution (Fig. 4a).

Classifying phenotypic convergence events by spatial context revealed that such cases tend to occur in pairs of clades with non-overlapping geographical distributions (Fig. 4b; see Methods). We also assessed whether similarity in foraging niches predicted evolutionary convergence events in the two most heterogeneous trophic groups (aquatic predators and terrestrial invertivores). In these diverse niches, we found that convergence among pairs of families using the same foraging techniques and substrates occurred far more often than predicted by chance (Fig. 4c). A key role for both geographical isolation and ecological similarity is consistent with the view that macroevolutionary convergence is driven by adaptation to vacant ecological niches<sup>47</sup>. Thus, the Neotropical region is home to arboreal frugivorous toucans (Ramphastidae) and ground-dwelling invertivorous antpittas (Grallariidae), which are replaced in the Palaeotropics by hornbills (Bucerotidae; Fig. 5a) and pittas (Pittidae; Fig. 5b), respectively. A minority of families, such as Swallows (Hirundinidae) and Swifts (Apodidae), appear to have converged despite broad spatial overlap (Fig. 5c), although it remains plausible that the early stages of convergence occurred in geographical isolation.

By tracing evolutionary trajectories through morphospace, we can visualise the likely history of convergence events according to a global phylogenetic tree<sup>41</sup>. These reconstructions show that, within matched family pairs, each clade has on average evolved a distance equivalent to one-third the span of total avian morphospace before arriving at its current position (Fig. 5a-c, Extended Data Fig. 13). In some cases (illustrated in Fig. 5a), family pairs have followed largely parallel trajectories, while in others (Fig. 5b-c) convergence has occurred from different points in morphospace, such that the current gap between families is substantially narrower than it was in the past.

A corollary of widespread convergent ecological adaptation to geographically segregated vacant niche space is that species occupying a given niche will cluster together in morphospace regardless of their geographic origins. To reveal this global mapping of form to function, we partitioned the avian hypervolume into biogeographic realms (see Methods). We found that each trophic niche has the same morphological signature worldwide, highlighting the repeatability of convergence events across multiple evolutionary arenas (Fig. 6).

## Conclusions

The connection between avian morphospace and trophic niches provides compelling evidence of widespread deterministic convergence in a diverse multitrophic assemblage<sup>27</sup>. Our analyses reveal that the predictable patterns of niche filling observed among individual lineages<sup>26,48</sup>, or in more localized settings<sup>47,49</sup>, are part of a grander evolutionary dynamic operating across entire classes of organisms at a global scale. This pervasive convergent evolution of morphological traits overrides the imprint of phylogenetic history in structuring avian niche space, reducing the power of phylogenetic biodiversity metrics to predict ecological function<sup>50</sup> unless combined with other information about traits. We have demonstrated that a minimum of four independent morphological trait axes are required to predict variation in avian trophic niches, calling into question the validity of trait-based macroecological analyses assessing functional diversity on the basis of fewer morphological trait dimensions (e.g. body mass). We also show that continuous morphological variables can predict much more subtle fine-scale variation in dietary and behavioural niches than can be achieved using standard niche categories (e.g. diet).

More generally, these findings have relevance to multiple environmental research programmes and policy frameworks, many of which have taken on increased urgency in light of rapid declines in animal diversity and abundance<sup>3,4</sup>. The avian trait space presented here—based on the most complete sample of morphological variation for any major taxon—provides a highly resolved template linking species traits to ecological function. Trait variation within any avian trophic guild, or clade, or indeed any historical, contemporary or predicted future bird community, can be mapped onto this template and interpreted in the context of regional or global patterns. In practical terms, this resource paves the way to a new generation of functional and behavioural diversity indicators for use in setting and measuring progress towards international conservation targets, understanding functional effects of extinction<sup>51</sup>, and evaluating how animal communities assemble and respond to change<sup>16,29,52</sup>.

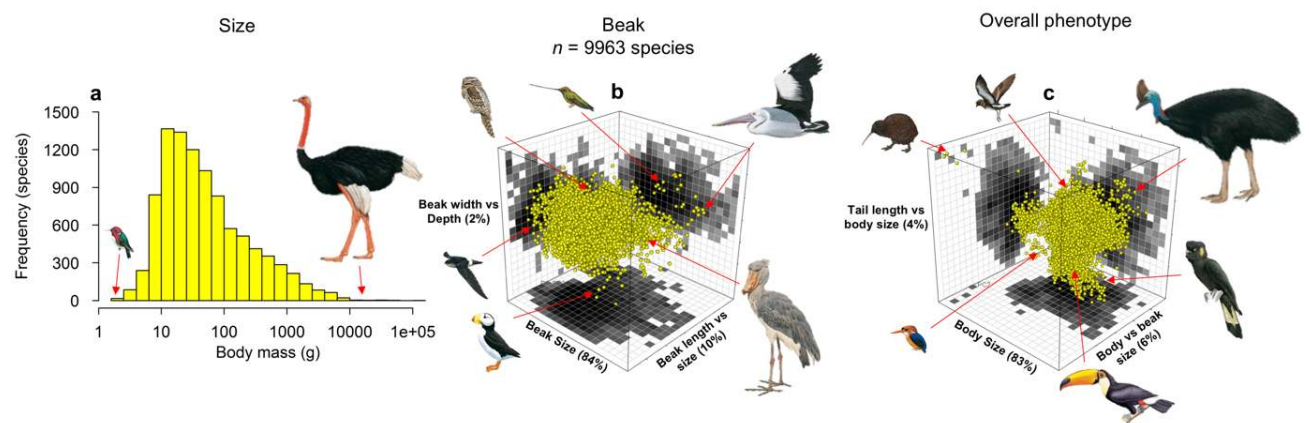


**Figure 1. The avian morphospace.** **a**, Distribution of avian body masses from the lightest (*Mellisuga helenae*, 2g) to the heaviest species (*Struthio camelus*, 111kg). **b**, Variation in beak shape, a key trait related to resource use. The first three dimensions of beak space capture variation in beak size (PC1), relative beak length (PC2) and ratio of beak depth to width (PC3). **c**, A three-dimensional morphospace combining data on body mass, beak, wing, tail and tarsus. Axis labels indicate the proportion of variance explained. The density of species is projected onto each two-dimensional plane. Data are shown for 9,963 species, representing >99% of all birds.

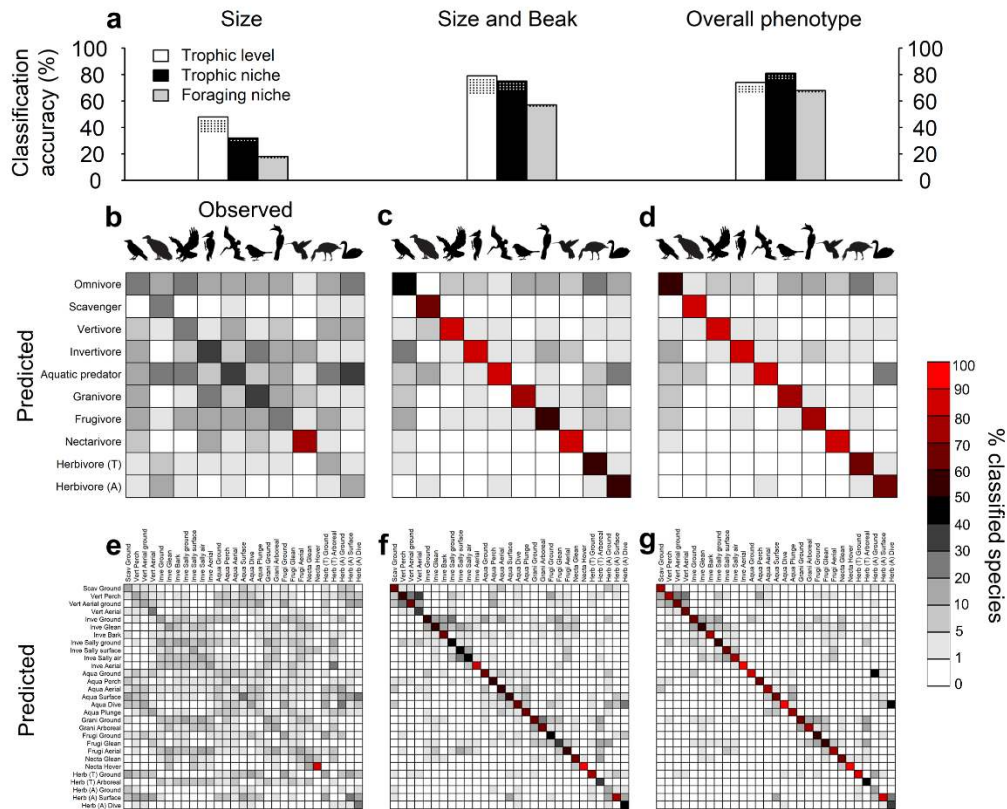


**Figure 2. Trophic structuring of multidimensional morphospace.** **a**, Mean accuracy (%) of a Random Forest model predicting trophic level, trophic niche and foraging niche for all birds ( $n = 9,963$  species) on the basis of body size (mass), size and beak traits, or the full nine-dimensional morphospace. Stippling indicates improvement in predictive accuracy after omitting omnivores (see Methods). **b-g**, Confusion matrices show predictions for each trophic (**b-d**) and foraging niche (**e-g**). Diagonal elements of each matrix indicate correct matches between predicted and observed niches; off-diagonal elements indicate misclassification. Red = high levels of accuracy (diagonal) or misclassification (off-diagonal).

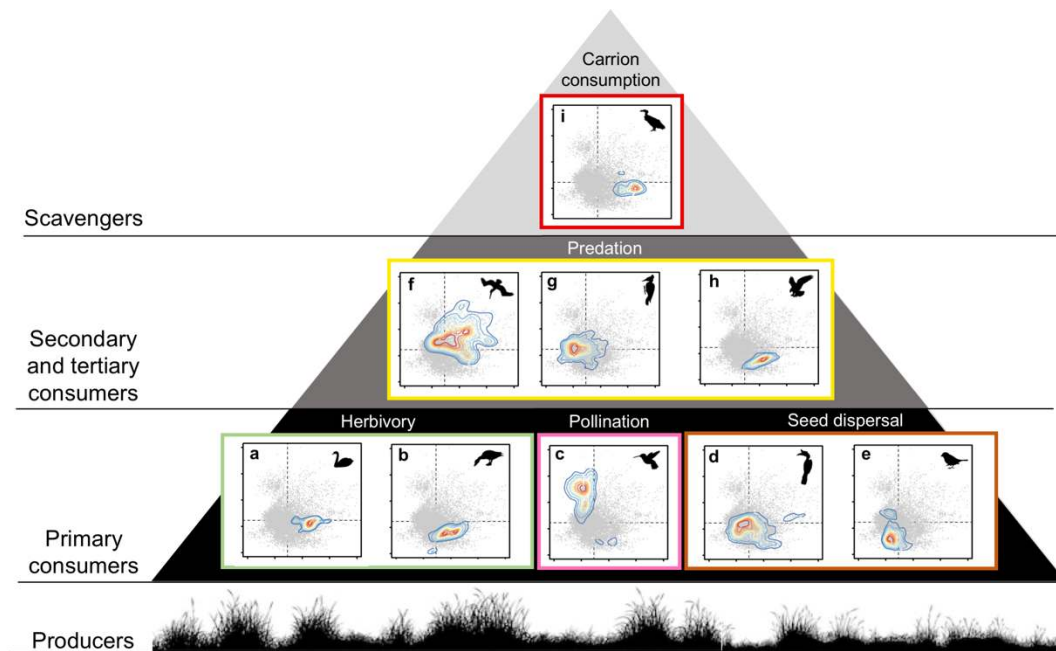
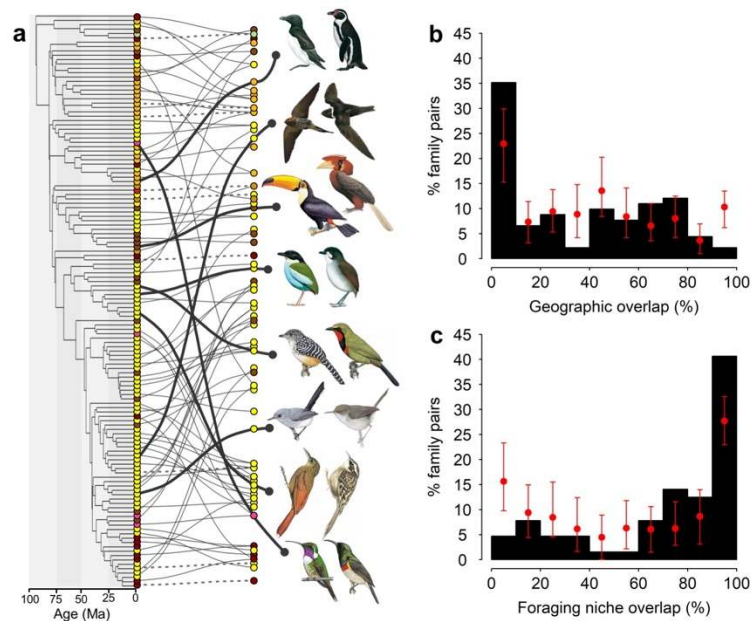


**Figure 3. Partitioning of avian morphospace across trophic levels and niches.**

Heterotrophic consumers shape the biosphere through numerous feedbacks on nutrient cycling and productivity<sup>2</sup>. Here we illustrate the complexity of avian ecological function as a multitrophic pyramid built on a foundation of autotrophic producers (plants), which are exploited directly by aquatic herbivores (**a**), terrestrial herbivores (**b**), nectarivores (**c**), frugivores (**d**), granivores (**e**), and indirectly by aquatic carnivores (**f**), terrestrial invertivores (**g**), terrestrial vertivores (**h**), and scavengers (**i**). Within each trophic niche, the first two dimensions of beak morphospace, capturing variation in beak size (PC1) and shape (PC2), are plotted against total beak variation of 9,963 species, representing >99% of all birds (light grey). Contours indicate density of species; warmer colours indicating higher density. Omnivores are not shown.



374

375 **Figure 4. Scale and context of macroevolutionary convergence in birds.** a, Lines  
 376 connect phenotypically matched families ( $n = 91$  pairs) spanning the avian evolutionary  
 377 tree. Exemplars highlighted with bold lines; sister clades with dashed lines. Tree tips are  
 378 coloured according to the predominant trophic niche (see Fig. 3). Matched family pairs  
 379 are not randomly distributed in relation to (b) geographic ( $n = 91$  pairs) and (c)  
 380 foraging niche overlap ( $n = 64$  pairs), with most cases having disjunct geographical  
 381 distributions and similar foraging niches. Red points and whiskers show the expectation  
 382 (median and 95% confidence interval) under a null model of trait evolution (see  
 383 Methods).

384

385

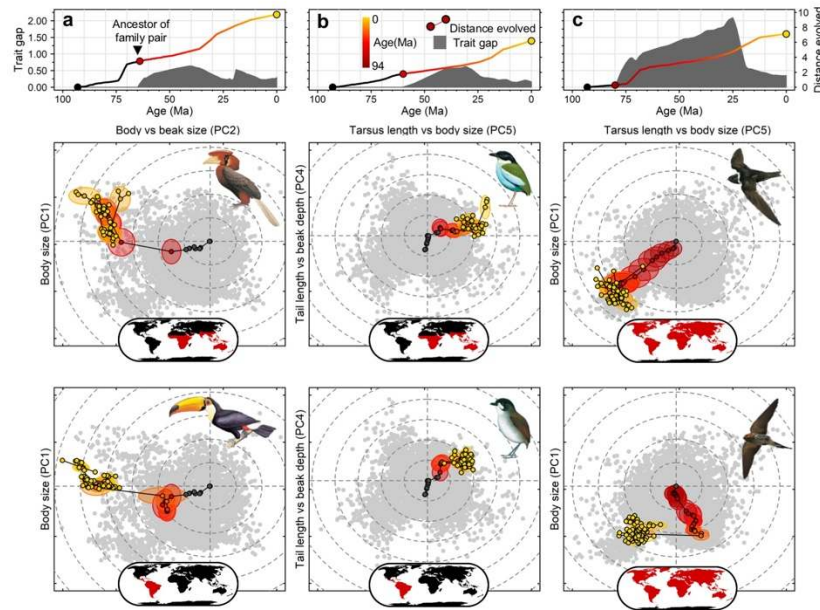


**Figure 5. Convergent evolutionary trajectories through avian morphospace.** To

illustrate the probable history of convergence events, data from ancestral trait reconstructions are shown for three exemplar pairs of convergent avian families (**a**, top: *Bucerotidae*; bottom *Ramphastidae*; **b**, top: *Pittidae*; bottom: *Grallaridae*; **c**, top: *Apodidae*; bottom: *Hirundinidae*). Uppermost panels show the cumulative phenotypic distance travelled by each family pair through morphospace, and the corresponding phenotypic gap between families. Phylomorphospace plots (lower panels) show the position of ancestral nodes within each clade (transition from yellow to red indicates increasing time before present, Ma) and prior to divergence of the family pair (grey). Size of discs around nodes indicates uncertainty in trait reconstruction. Nodes leading to other lineages are not shown. Maps show global distribution of each family in relation to biogeographic realms (see Fig. 6).

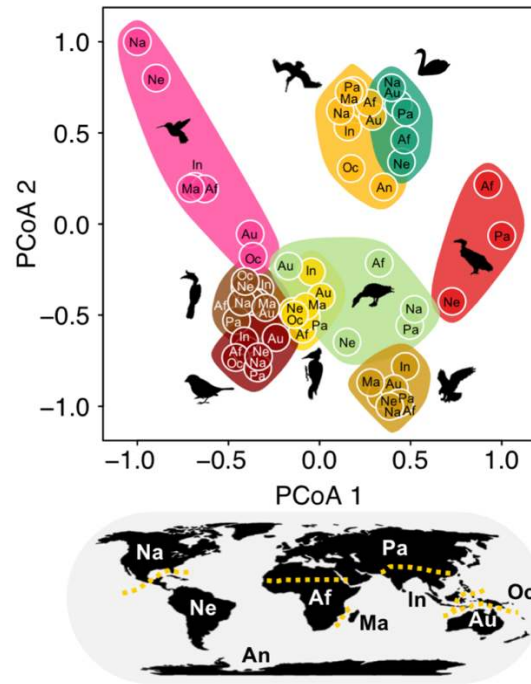


**Figure 6. The global mapping of form to function across birds.** Clustered points along each principal coordinate axis (PCoA) show the relative morphological similarity between trophic niches from different ecological theatres (biogeographic realms) based on the average pairwise distance between species ( $n = 9,963$  species) in nine-dimensional morphospace (see Methods). Individual trophic niches are omitted from realms in which they are absent or rare ( $<6$  species).

## Methods

### Morphological trait data

We assembled a database of morphometric measurements from 52,870 live caught individuals and preserved museum skins, of which 2,288 specimens were from existing published databases<sup>53,54</sup>. In total, our database represents 9,963 of the 9,993 extant species (99.7%) recognized in the global avian taxonomy utilized by Jetz et al.<sup>41</sup>. For each individual, we measured eight traits (generally to the nearest 0.1 mm): beak length (from tip to skull along the culmen, and to the nares), beak width and depth at the nares, tarsus length, wing length, first secondary length, and tail length (see Extended Data Fig. 1 and Extended Data Table 1 for further descriptions). We obtained measurements from at least four adult individuals from each species where possible (two from each sex; mean total = 5.3 individuals). Sampling was conducted by 93 researchers across 65 museum collections worldwide using a standard protocol (see Supplementary Information). To assess repeatability, we compiled measurements by different researchers on the same specimens ( $n = 2752$  individuals of 2523 species). Repeated measures were highly concordant as measurer identity accounted for only 0.74% of total trait variance in this dataset (Extended Data Fig. 2; see Supplementary material for details). We extracted estimates of mean species body mass (g) from Wilman et al.<sup>40</sup>, largely based on the compilation by Dunning<sup>55</sup>. To match the species level resolution of our ecological niche data (see 'Ecological niche data' for details), we calculated mean trait values for each species. This is justifiable because most of the variance in trait values occurs between (98.25%) rather than within (1.75%) species (Extended Data Table 1; see Supplementary material for details). We performed a principal components (PC) analysis on the log-transformed mean species trait values. We centred and rescaled each phenotypic trait to unit variance before performing two separate PC analyses using (1) the four beak measurements (beak length at nares and culmen, beak width and depth at nares) and (2) all nine phenotypic traits (Extended Data Fig. 3). We visualised the distribution of species throughout nine-dimensional morphospace by calculating the density of species within concentric shells with a width of one morphological unit (Extended Data Fig. 4).

### Ecological niche data

For each species, we scored the proportion of its diet obtained from three trophic levels (primary consumer; secondary/tertiary consumer; scavenger) and nine trophic niches (aquatic herbivore; terrestrial herbivore; nectarivore; granivore; frugivore; aquatic predator; invertivore; vertivore; scavenger) encompassing the major resource types utilized by birds (Extended Data Fig. 5a). Our scoring of species diets is primarily based on data from Wilman et al.<sup>40</sup>, extensively updated and re-organized based on recent literature. For instance, we classified species eating any kind of aquatic prey as aquatic predators, whereas in Wilman et al.<sup>40</sup> species feeding on aquatic and terrestrial invertebrates were grouped together (e.g. flamingos with warblers). Based on these dietary scores we assigned species to the trophic level from which they obtained at least 70% of their resources, with species utilizing multiple trophic levels in relatively equal proportions classified as ‘omnivores’<sup>56</sup>. Similarly, we assigned species to the trophic niche from which they obtained at least 60% of their resources (this lower threshold was chosen due to the larger number of trophic niche categories<sup>56</sup>). Species utilizing multiple niches, within or across trophic levels, in relatively equal proportions were classified as ‘trophic generalists’. Although not all omnivores are trophic generalists, and vice versa, there is nonetheless broad overlap, and for simplicity we use the term ‘omnivore’ when referring to both categories together.

Following the standardized protocol outlined in Wilman et al.<sup>40</sup>, we used the extensive literature on avian feeding ecology and behaviour (e.g.<sup>57</sup>) to quantify for each species the relative use of 31 different foraging niches (scored in 10% intervals), describing different combinations of diet, foraging manoeuvre and substrate (Extended Data Fig. 5b-c). These foraging niches expand on previous guild classifications<sup>31,32,34,58-61</sup> to reflect the wider taxonomic and ecological scope of our analysis. Based on these scores, we assigned each species occupying a specialist trophic niche (i.e. excluding omnivores) to the foraging strategy by which it accessed at least 60% of its dominant resource type. Two foraging niches (ground and arboreal gleaning vertivores) were each represented by only six species and so were excluded. Species utilising multiple foraging strategies in relatively equal proportions were classified as ‘foraging generalists’, thus providing a total of 30 foraging niches used in our analysis. Further descriptions of each foraging niche, and the assignment of species to each category, are provided in Extended Data Table 4.

## **Phylogenetic data**

To explore the evolutionary basis of form-function relationships, we used the time-calibrated molecular phylogeny of Jetz et al.<sup>41</sup> using the Hackett et al.<sup>62</sup> backbone. To ensure reliable estimates of evolutionary parameters, we restricted our phylogenetic analyses to the  $n = 6,666$  species with morphological data and for which branch lengths were estimated on the basis of genetic data. Because the evolutionary models we use are computationally expensive to fit to the entire avian phylogeny, we based our analysis on the maximum clade credibility (MCC) tree generated from across 1,000 trees sampled at random from the posterior distribution using TREEANNOTATOR (included in BEAST v.1.6.1)<sup>63</sup>.

## **Geographic data**

Range maps of species breeding distributions were obtained from Birdlife International (<http://www.birdlife.org/datazone/home>). Owing to the taxonomic lumping or splitting of various lineages, there are differences in the species classification used by IUCN and Jetz et al.<sup>41</sup>. We aligned the IUCN dataset with that of Jetz et al.<sup>41</sup> by editing species range maps in ArcMap v 10.3<sup>64</sup> based on published information on geographical ranges of relevant taxa<sup>57</sup>. Species ranges were then extracted onto an equal area grid (Behrmann projection) with a resolution of 110 km ( $\approx 1^\circ$  at the equator).

## **Quantifying the match between traits and niches**

We tested whether species ecological niches can be predicted on the basis of species traits using Random Forest (RF) models<sup>65</sup> implemented using the R<sup>66</sup> package 'randomForest'<sup>67</sup>. This method is suitable for matching traits to ecology because it makes minimal assumptions about the shapes of species niches and can accommodate interactions across multiple trait axes. RF models use an ensemble of decision trees to partition feature space (i.e. morphospace) into a set of non-overlapping rectangular hypervolumes within which impurity in ecological niches is minimised (Supplementary Fig. 1). Each internal node in a tree thus corresponds to a split along one randomly selected dimension of morphospace, with each terminal node corresponding to a unique rectangular hypervolume. Each decision tree in the RF provides a 'vote' on the identity of a species' ecological niche based on its position in morphospace. We used the majority vote across trees to predict the ecological niche of species and then calculated

the proportion of species correctly assigned to each niche. Throughout we report overall model predictive performance as the mean classification accuracy across ecological niches. Model parameters, including the number of trees ( $n = 500$ ) and the number of random traits to sample at each node ( $n = 2$ ), were selected based on initial sensitivity tests.

Because species are highly unevenly distributed across ecological niches, we randomly up-sampled or down-sampled each niche to an equivalent number of species before fitting the models ( $n = 5000$ , 2000 and 1000 species for trophic levels, trophic niches and foraging niches respectively). To provide unbiased estimates of predictive performance, we used 5-fold cross validation. We randomly split our data into five equal sized sets, maintaining the same relative frequency of each ecological niche within each set. We trained a model on 80% of the data ('training set') and used this to predict species niches in the remaining 20% of the data ('test set'), repeating this five times, once for each partition. To account for stochasticity in model fit arising the random partitioning of the dataset during cross-validation, we fitted eleven replicate models and used the modal prediction for each species. We compared the predictive performance of RF models including: (1) only body mass, (2) body mass and PC scores based on all beak measurements (length, width and depth), and (3) PC scores based on all nine phenotypic traits.

### **Sensitivity tests of trait-niche matching**

While the RF model detects a strong statistical match between traits and ecological niches (Fig. 2), it is possible that this accuracy is only achieved through a highly complex mapping of form to function. For example, each niche could be comprised of multiple, widely scattered clusters in morphospace representing a series of unique evolutionary radiations. If one member of each cluster is included in the training dataset, we may infer a high statistical predictability of trophic niches, despite the link between morphology and ecology being unpredictable (i.e. not repeatable) in an evolutionary sense<sup>26</sup>. We examined this by (1) re-fitting a RF model constraining the number of terminal nodes permitted in each tree, and (2) repeating our analysis using Linear (LDA) and Mixture Discriminant Analysis (MDA). Discriminant Analysis is widely used for matching variation in ecology and morphology based on restrictive assumptions about the shape of ecological niches. Unlike our RF model, LDA assumes that each niche

corresponds to a single multivariate normally distributed morphological cluster, with equal variance across niches. MDA relaxes these assumptions by allowing each niche to be modelled by a Gaussian distribution of subclasses, with an equal covariance structure across subclasses.

First, we found that even when RF tree size is strongly constrained (e.g.  $n = 20$  terminal nodes), predictive accuracy remains high, indicating that each trophic niche can be well described by one or a few rectangular hypervolumes (Supplementary Fig. 2). Second, despite their restrictive assumptions, the LDA and MDA predicted specialist trophic niches with a 71% and 80% accuracy, respectively (Extended Data Fig. 6). Thus, additional analyses support high predictability of ecological niches, indicating that the strong match between traits and ecology does not arise from over-fitting of the RF model and instead reflects a relatively simple one-to-one mapping of morphology to ecological niches.

Simulations show that, depending on the shape and arrangement of ecological niches in morphospace, MDA and LDA may underestimate the true match between traits and ecological niches (Supplementary Fig. 3). Specifically, when niches occur as disjunct clusters in morphospace, as observed in some smaller species radiations (e.g. *Anolis* lizards<sup>47</sup>), then LDA and MDA accurately predict niche identity (Supplementary Fig. 3a-b). However, when niches have irregular shapes that closely abut in morphospace, as in our empirical dataset (Fig. 3), species along the boundaries of each niche are likely to be misclassified leading to a lower predictive accuracy (LDA = 84%; MDA = 95%) (Supplementary Fig. 3c-d). In contrast, a RF model can readily incorporate close non-linear relationships, providing a more robust estimate of the match between morphology and ecology. We therefore focus our analysis on the results from the RF model.

### **Phylogenetic null model of trait-niche relationships**

The predictable relationship between traits and ecological niches may simply reflect shared phylogenetic ancestry. We assessed this possibility by comparing the empirical estimates of niche predictability to those expected under an evolutionary null model. Keeping the trophic niche of each species fixed, we simulated morphological trait values according to a Brownian motion model of trait evolution applied to the avian phylogenetic tree (see section 'Phylogenetic models of Brownian trait evolution' for

details)<sup>68</sup>. This null model allowed us to quantify the similarity in species traits expected due to phylogenetic relatedness in the absence of ecological adaptation. We fitted a RF model to each of 100 replicate simulated trait distributions in order to calculate the expected predictability of overall niche space and each individual trophic niche (Extended Data Fig. 11a). We repeated this analysis using MDA and LDA as alternative methods for matching traits to niches and obtained similar results (Extended Data Fig. 11b-c). As a further test, we assessed whether species sharing the same trophic niche are more densely packed in trait space than expected under the evolutionary null model by comparing the mean pairwise Euclidian trait distance between species within each trophic niche to that expected across 1000 simulations of the null model (Extended Data Fig. 12).

### **Phylogenetic models of Brownian trait evolution**

We parameterized the null model of Brownian trait evolution according to the empirical rates of trait evolution estimated across the avian phylogenetic tree using BAMM<sup>69,70</sup>. This modelling framework uses reversible jump Markov chain Monte Carlo (MCMC) to fit a set of distinct macro-evolutionary regimes across the phylogenetic tree, the number, location and parameters of which are estimated from the data. Each regime may be characterized by a different rate and dynamic of trait evolution, including either increasing or decreasing rates through time. Unlike many studies, we are not specifically interested in these estimated parameters *per se*, and instead simply use them to parameterize our null model simulations to account for the potentially complex dynamics of avian phenotypic evolution.

We fitted this model separately to each of our nine PC trait axes to estimate marginal densities of phenotypic rates on each branch of the avian phylogeny. Sensible priors on rate parameters were assigned using the `setBAMMpriors` functions. We ran the MCMC simulation for 600 million generations, sampling the parameters every 80,000 generations. We discarded the first 10% of samples as burn-in and assessed convergence by calculating the effective sample size (ESS) of the model log-likelihood and the estimated number of macro-evolutionary regime shifts. ESS for each trait was consistently above the recommended value of 200. We used the mean marginal rate configuration across the phylogeny to parameterise the simulations.

## Quantifying the dimensionality of trophic niche space

To quantify the dimensionality of trophic niche space, we fitted RF models to morphospaces consisting of one to nine trait dimensions, exploring all possible combinations of PC trait axes ( $n = 511$  trait combinations for nine traits) (Extended Data Fig. 7a). We repeated this analysis using phylogenetically corrected principal component scores, obtaining very similar results (Extended Data Fig. 7b). For each level of dimensionality, we identified the combination of trait axes that provided the highest mean niche predictability (Extended Data Fig. 7). In one dimension, PC1 is the optimal trait axis. However, in higher dimensions the identity of the optimal trait axes does not simply correspond to their relative contribution to total phenotypic variance (Extended Data Fig. 7). For instance, in three dimensions, trophic niche space is best described by PC1, PC3 and PC4 rather than PC2 (Extended Data Fig. 8a). In general, trait axes accounting for only a minor fraction to the total phenotypic variance contribute disproportionately to defining ecological niche space.

Using the maximum predictive accuracy at each level of morphospace dimensionality, we calculated the dimensionality of trophic niche space ( $D_{\text{Total}}$ ) according to Levene's index<sup>71</sup>,

$$D_{\text{Total}} = \frac{1}{\sum p_i^2}$$

where  $p_i$  is the proportion of the maximum predictive accuracy (across all trait combinations) accounted for by dimension  $i$ . We applied the same approach to calculate the dimensionality of each individual trophic niche and also foraging niche space.

The core trait dimensions identified using these estimates of dimensionality (Extended Data Fig. 8c-d) varied across niches in ecologically informative ways. For instance, it makes sense that PC7 forms one of three core axes of the granivore (seed-eating) niche because it describes the ratio of beak depth to width, with higher values corresponding to a stronger bite force and ability to crush seeds<sup>39</sup>. Similarly, one of three core axes of the aquatic predator niche is PC8, a correlate of wing pointedness, with higher values corresponding to greater soaring ability and flight efficiency<sup>72</sup>.

## Sensitivity tests of niche dimensionality

To assess the robustness of our estimates of niche dimensionality  $D$ , we performed multiple sensitivity tests. First, we repeated our analysis using synthetic morphological axes generated from a phylogenetic PCA that accounts for the non-independence of species<sup>73</sup>. Estimates of niche dimensionality ( $D_{\text{Total}} = 4.4$ ) and predictive accuracy (81%) obtained using this method were very similar to those based on phylogenetically-uncorrected PC axes (Extended Data Fig. 7a-b). Second, rather than a RF model we used LDA and MDA to predict trophic niches. Estimates of trophic niche dimensionality ( $D_{\text{Total}}$ ) vary from  $D_{\text{Total}} = 3.3$  for MDA to  $D_{\text{Total}} = 6$  for LDA, with a RF model providing an intermediate estimate of  $D_{\text{Total}} = 4.4$  (Extended Data Fig. 10). At the scale of foraging niches, estimates of dimensionality were more constrained varying from  $D_{\text{Total}} = 5.6$  (RF and MDA) to  $D_{\text{Total}} = 6$  (LDA) (Extended Data Fig. 10). Thus, all models agree that (1) trophic niche space is minimally described by at least four complete trait dimensions and that (2) when niches are resolved at a much finer scale (i.e. foraging behaviours and substrates), dimensionality increases only marginally, with niche space described with six or fewer trait dimensions. Given the higher predictive accuracy of the RF model and the known sensitivity of MDA and LDA to niche shape we consider the RF estimates to be the most robust (see ‘Sensitivity tests of trait-niche matching’, Supplementary Fig. 3).

Our trait sampling generates imperfect predictions of trophic niches, suggesting that additional trait axes may be required to fully describe niche space, leading to potentially higher estimates of dimensionality. To explore this possibility, we simulated how total niche dimensionality ( $D_{\text{Total}}$ ) changes when the remaining variation in niches left unexplained by our nine-dimensional morphospace is equitably divided among an additional number of hypothetical trait dimensions. Simulations show that even with the addition of many hypothetical trait axes (e.g.  $n = 100$  trait dimensions), our estimate of trophic niche dimensionality increases only marginally ( $D_{\text{Total}} = 6.1$  versus 4.4, Extended Data Fig. 9a).  $D_{\text{Total}}$  is robust to this proliferation of trait dimensions because so much variation in trophic niches is explained by our existing nine-dimensional morphospace (Extended Data Fig. 7a). Estimates of foraging niche dimensionality are potentially more sensitive to the inclusion of additional trait axes, with our simulations suggesting an upper bound of  $D_{\text{Total}} < 11$  (Extended Data Fig. 9b). We note, however, that these simulations are likely to overestimate the potential increase in dimensionality from measuring additional traits. For instance, if some variation in ecology occurs independently of traits or if there are differences in the amount of

ecological variation explained by hypothetical trait dimensions, this leads to substantially smaller increases in  $D_{\text{Total}}$  (Extended Data Fig. 9b). Thus, our simulations should be viewed as providing an upper bound on niche dimensionality.

### **Identifying phenotypically matched families**

To identify clades with similar ecologies that are most similar in their functional traits, we assigned avian families to one of three functional groups: (1) primary consumers, (2) terrestrial secondary/tertiary consumers, and (3) aquatic secondary/tertiary consumers. We restricted the analysis to families containing more than 5 species with both genetic and morphological data ( $n = 132$ ). Because relatively few large families were aquatic primary consumers or scavengers, these groups were lumped with terrestrial primary consumers and terrestrial secondary/tertiary consumers, respectively. Within each of these functional groups, we identified phenotypically matched pairs of families by fitting a RF model predicting family identity on the basis of morphological traits and then calculating the mean species proximity scores for each pairwise combination of clades. These scores indicate the proportion of times a species in a clade is assigned to the same rectangular hypervolume as a species from another clade. This metric of proximity has an advantage over standard distance-based measures (e.g. Euclidian distances) because it does not require any assumptions regarding the relative importance of different trait axes in discriminating between families. Instead, this information is learnt from the data. In total, we identified  $n = 91$  unique family pairs (41 reciprocally matched pairs were only counted once in the analysis) (Supplementary table 1).

### **Reconstructions of ancestral traits**

To visualise how matched family pairs have evolved similar trait values, we used the branch and trait specific rate estimates obtained from our BAMM analysis to reconstruct trait values at each node in the phylogenetic tree as well at 1 million year (myr) time intervals along each branch<sup>74</sup>. For each time step, we quantified the mean position of each family along each trait axis, and summed the Euclidian distance between these successive time points to estimate the total distance evolved across morphospace by each family since they diverged<sup>75</sup>. To visualise the evolutionary trajectories of selected families through morphospace (Fig. 4b-d), we also calculated the

trait gap (i.e. 5% quantile of minimum pairwise distances) between each family at each 1myr time interval<sup>75</sup>.

Different family pairs occupy different trophic and foraging niches and these niches are defined by different sets of traits (Extended Data Fig. 8). When calculating phenotypic distance metrics, we therefore selected the two trait axes that best describe the niche of each family pair (Supplementary table 1). These trait axes were identified using the mean ranking of variable importance scores across the two families from the RF model. To compare distance metrics based on different combinations of trait axes, we rescaled current and ancestral species trait values to unit variance prior to calculating phenotypic distances. We express these distances as a proportion of the total span of avian morphospace, calculated as the diameter of a circle centred on the centroid of morphospace and containing 95% of species (Extended Data Fig. 13).

### **The ecology and geographic distribution of phenotypically matched clades**

To explore the geographic and ecological context of convergence, we quantified spatial overlap and similarity in foraging behaviour of families within matched pairs (Supplementary table 1). Spatial overlap between families ( $n = 91$  pairs) was quantified using the summed proportion of each species geographic range occurring in each of nine biogeographic realms<sup>76</sup>. Foraging niche overlap between families of aquatic predators and invertivores ( $n = 64$  pairs) was quantified using the summed proportional use of each foraging niche. Spatial and foraging overlap were scored using Schoener's D statistic (here denoted by the symbol  $S$  to distinguish from our Dimensionality metric),

$$S(p_X, p_Y) = 1 - \frac{1}{2} \sum_i |p_{X,i} - p_{Y,i}|$$

where  $p_{X,i}$  (or  $p_{Y,i}$ ) is the proportional use of region/niche  $i$  by species  $X$  (or  $Y$ ). Values of  $S$  vary from 0 (no overlap) to 1 (complete overlap) and were multiplied by 100 to report overlap scores for each family pair from 0 to 100% (in 10% intervals).

If families are restricted to single biogeographic realms or foraging niches, then many family pairs would be expected to show little spatial or ecological overlap simply by chance. We therefore compared the observed frequency of spatial and foraging

overlap to that expected under 100 replicate simulations of our phylogenetic null model, in which matched family pairs are generated through a process of complex Brownian trait evolution (see section ‘Phylogenetic null models of trait-niche relationships’ for details).

To visualize the effects of these non-random evolutionary dynamics, we generated a matrix of pairwise trait distances between the species in the full nine-dimensional morphospace. We calculated the mean distance between species in each combination of trophic niche and biogeographic realm and used Nonmetric Multidimensional Scaling to translate this distance matrix onto two orthogonal principal coordinate axes.

#### **Data availability**

All geographic and phylogenetic data are publicly available. Morphological data and ecological niche assignments will be made available with the final accepted version of the article.

#### **Code availability**

All custom scripts will be made available with the final accepted version of the article.

**Extended Data Table 1.** Description of species traits and % of variance attributed to intraspecific differences (from a variance components analysis).

Trait (mm)	Description	% variance within species
Beak length (tip-to-nares)	Distance from the anterior edge of the nostrils to the tip	1.39
Beak length (culmen)	Distance along the culmen from the base of the beak to the tip	1.71
Beak width	Width of beak at the anterior edge of the nostrils	2.49
Beak depth	Vertical height of beak at the anterior edge of nostrils	1.62
Tarsus length	Distance from the middle of the rear ankle joint, i.e. the notch between the tibia and tarsus, to the end of the last scale of the acrotarsium	1.71
Wing length (mm)	Distance between the carpal joint to wing tip	0.72
Secondary length (mm)	Distance between the carpal joint to the tip of the first secondary feather	1.33
Tail length (mm)	Distance from the tip of the longest rectrix to the point at which the two central rectrices protrude from the skin	2.99
Body mass (g)	Mass	NA

Estimates of intraspecific variation are not available for body mass.

**Extended Data Table 2.** Trait loadings for beak space and % of variance accounted for by each principal component axis ( $n = 9963$  species).

Trait	PC1	PC2	PC3	PC4
Beak length (culmen)	0.46	0.47	-0.01	-0.75
Beak length (tip-to-nares)	0.52	0.55	0.02	0.66
Beak width	0.47	-0.46	0.76	-0.01
Beak depth	0.55	-0.52	-0.65	0.02
Variance %	84.2	13.0	1.7	1.1
Cumulative variance	84.2	97.2	98.9	100

**Extended Data Table 3.** Trait loadings for phenotype space and % of variance accounted for by each principal component axis ( $n = 9963$  species).

	PC1	PC2	PC3	PC4	PC5	PC6	PC7	PC8	PC9
Beak length (culmen)	0.22	-0.42	0.30	-0.26	0.08	-0.10	0.07	0.01	0.77
Beak length (tip-to-nares)	0.23	-0.67	0.23	-0.26	0.05	0.08	-0.04	0.06	-0.60
Beak width	0.23	-0.26	-0.37	0.41	0.01	0.06	0.75	-0.11	0.01
Beak depth	0.28	-0.29	-0.39	0.47	0.13	-0.05	-0.65	-0.06	0.11
Tarsus length	0.23	0.26	0.13	-0.06	0.86	0.00	0.06	-0.34	-0.09
Wing length	0.26	0.10	-0.15	-0.28	-0.30	0.66	-0.10	-0.53	0.07
Tail length	0.21	0.07	-0.58	-0.56	-0.06	-0.54	0.02	-0.07	-0.06
Secondary length	0.25	0.14	-0.26	-0.18	0.22	0.44	0.02	0.76	0.07
Body mass	0.74	0.34	0.36	0.19	-0.31	-0.23	0.00	0.10	-0.10
Variance %	83	6.1	3.8	3.2	2.1	0.8	0.5	0.3	0.2
Cumulative variance	83	89.2	93	96.2	98.3	99.1	99.6	99.9	100

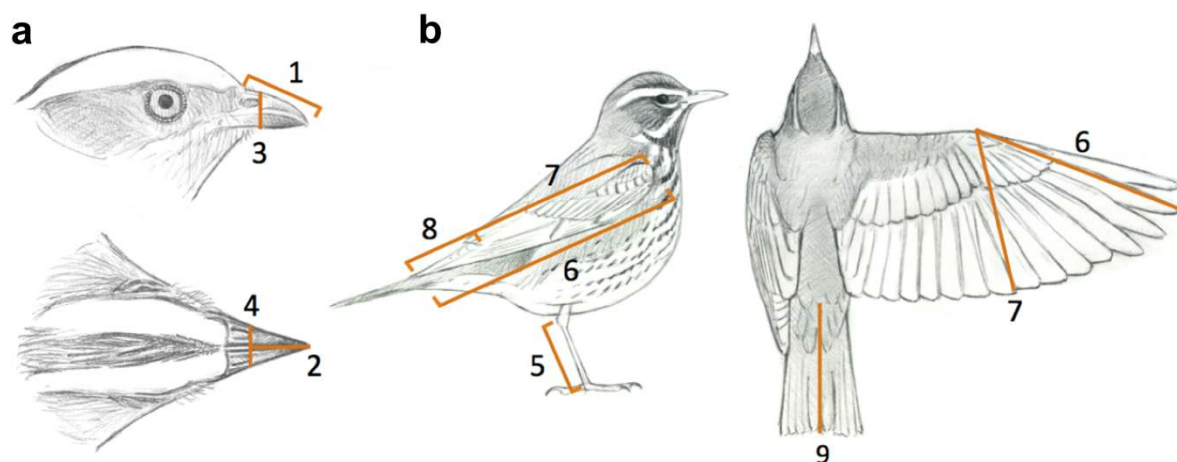
**Extended Data Table 4.** Description of foraging niches within specialist trophic niches.

<b>Scavenger</b> ( <i>n</i> = 22)	<b>Ground (SCG, <i>n</i> = 22)</b> – species eating carrion (dead animal or fish remains) on the ground (e.g. vultures).
<b>Invertivore</b> ( <i>n</i> = 4765)	<b>Aerial screen (IASC, <i>n</i> = 278)</b> – species capturing flying invertebrates on the wing (e.g. swallows, swifts). Often described as ‘hawking’. In contrast to ISA, IASC is characterized by continuous and extended flight with multiple items captured before landing.
	<b>Aerial sally (ISA, <i>n</i> = 317)</b> – species capturing flying invertebrates in mid-air, with the attack starting from a perch (i.e. branch, rock, fence post, telegraph wire, etc.) and then returning to a perch (e.g. jacamars, kingbirds, etc). ‘Hawking’ will sometimes refer to this category, but the key distinguishing feature is that only a single prey item is captured before returning to a perch.
	<b>Sally to substrate (ISS, <i>n</i> = 343)</b> – species capturing invertebrates (including arachnids, worms, molluscs, etc.) attached to the substrate (e.g. leaves, twigs, branches, rock faces, etc) following an aerial attack manoeuvre (e.g. flight, pounce, jump, hover).
	<b>Sally to ground (ISG, <i>n</i> = 245)</b> – species capturing invertebrates on the ground following an aerial attack manoeuvre (e.g. flying, gliding, dropping or pouncing) (e.g. chats, shrikes, kiskadee etc). The aerial manoeuvre may be followed by brief hopping toward prey (e.g. terns).
	<b>Glean arboreal (IGA, <i>n</i> = 1792)</b> – species capturing invertebrates attached to the substrate (e.g. leaves, twigs, branches, grass, bamboo, stems, hanging dead-leaves [not dead leaves on the ground] etc). No aerial attack manoeuvre is involved.
	<b>Glean bark (IGB, <i>n</i> = 339)</b> – species capturing invertebrates attached to or concealed within large branches and trunks of trees (e.g. woodpeckers, treecreepers, woodcreepers, wallcreepers, nuthatches, sittelas, nuthatches, vangas, etc., including honeyguides). This is distinguished from IGA by at least one criterion. First, the species employs specialized methods for moving over surfaces which are often, but not always vertical, vertical and too large to be gripped by the closed foot (including creeping, climbing or scaling). Second, the species extracts prey from in/under the bark using specialized methods (including hammering, probing or chiselling). Also includes species capturing insects from rock and cliff-faces (though not just on boulders [see IGG]), habitually perching on or clinging to large mammals and species that feed on honey and beeswax.
	<b>Glean ground (IGG, <i>n</i> = 1026)</b> – species capturing invertebrates on the ground. In contrast to ISG, the search and attack manoeuvres take place on the ground (e.g. thrushes). This includes species standing on the ground and gleaning insects from vegetation (e.g. tinamous or larks) but excludes species that jump or sally upwards to capture prey from vegetation (ISS) or the air (ISA). The ground is dry and thus excludes aquatic habitats (including beaches, estuaries, wetlands and marshes [see AQGR]).
<b>Aquatic predator</b> ( <i>n</i> = 757)	<b>Ground (AQGR, <i>n</i> = 314)</b> – species capturing invertebrates or vertebrates while standing in aquatic habitats (including beaches, estuaries, wetlands and marshes) (e.g. storks, herons, shorebirds). Prey may be captured on the ground or on/under water. This category includes species capturing aquatic prey (e.g. fish) or terrestrial prey in aquatic habitats (e.g. grasshopper).
	<b>Perch (AQPE, <i>n</i> = 44)</b> – species capturing invertebrates or vertebrates on/under water following a direct attack flight from a perch (e.g. kingfisher).
	<b>Aerial (AQAE, <i>n</i> = 87)</b> – species capturing invertebrates or vertebrates on/under water during continuous flight (including dipping, hovering, pattering, snatching). In contrast to AQPE, prey item is identified while flying (not from perch). The predators body may partially submerge but does not plunge beneath the surface (AQPL). Includes kleptoparasitic species capturing fish by chasing other piscivores and forcing them to regurgitate (e.g. skuas, frigatebirds).
	<b>Plunge (AQPL, <i>n</i> = 59)</b> – species capturing invertebrates or vertebrates by plunging under water following continuous flight. The predators body submerges

	entirely beneath the surface, with the prey captured either by the momentum of the plunge or following propelled swimming.
	<b>Surface (AQSU, <math>n = 73</math>)</b> – species capturing invertebrates or vertebrates on/under water whilst swimming on the water surface. In contrast to AQPE or AQAI there is no direct attack flight. The species may dip under the water but, in contrast to AQDI, contact with the surface is maintained.
	<b>Dive (AQDI, <math>n = 134</math>)</b> – species capturing invertebrates or vertebrates under water by diving from the surface (not the air, see AQPE and AQPL).
<b>Vertivore</b> ( $n = 311$ )	<b>Aerial screening (VASC, <math>n = 20</math>)</b> – species captures vertebrate prey during flight. Both predator and prey are in flight (e.g. peregrine, hobby, falcon)
	<b>Aerial to substrate (VAS, <math>n = 54</math>)</b> – species captures prey on branches or the ground by diving from the air, usually after circling or hovering in flight. Includes quartering flight (e.g. kestrels, kites, some owls).
	<b>Sally to substrate (VSS, <math>n = 190</math>)</b> – species captures prey on branches or the ground by diving from a perch (e.g. many owls, eagles).
	<b>Glean ground (VGG, <math>n = 6</math>)</b> – species capturing prey on the ground, including eggs in ground nests, while they themselves are also walking or running on the ground (e.g. secretary bird, seriemas, ground hornbills).
	<b>Glean arboreal (VGA, <math>n = 6</math>)</b> – species capturing prey from foliage, branches, epiphytes, cavities, bark or other arboreal substrate while perched on the substrate. There is no flight attack involved. This includes eating bird chicks from arboreal nests and drinking blood while perched on mammals (e.g. oxpeckers).
<b>Nectarivore</b> ( $n = 507$ )	<b>Aerial (NAE, <math>n = 318</math>)</b> – species feeding on nectar or other plant exudates (e.g. sap) while in flight (e.g. hummingbirds).
	<b>Glean (NGL, <math>n = 184</math>)</b> – species feeding on nectar or other plant exudates (e.g. sap) while perched, including nectar predators that pierce corollas (e.g. sunbirds, flowerpiercers). Species feeding on honey (e.g. honeyguides) included under IGB.
<b>Granivore</b> ( $n = 662$ )	<b>Granivore above-ground (GRA, <math>n = 185</math>)</b> – species foraging on seeds, grains and nuts taken from vegetation (e.g. trees, grass stems) while perched (e.g. seedeaters, finches).
	<b>Granivore ground (GRG, <math>n = 408</math>)</b> – species foraging on fallen seeds, grains and nuts collected from the ground. Including birds that eat grains by, on, and under water (e.g. partridges, pheasants, finches).
<b>Herbivore terrestrial</b> ( $n = 93$ )	<b>Above-ground (PA, <math>n = 13</math>)</b> – species foraging on leaves, buds, blossom, or other vegetation (except fruit, seeds and nectar). The food is taken from above ground, generally while the species is perching on branches or other stems. Generally, a small part of diet, except for the hoatzin, plantcutters.
	<b>Ground (PG, <math>n = 73</math>)</b> – species foraging on grass, leaves, buds, blossom, or other vegetation (not fruit or seeds) taken while the species is on the ground (e.g. geese). The vegetation may itself be off the ground.
<b>Herbivore aquatic</b> ( $n = 82$ )	<b>Aquatic ground (PAQGR, <math>n = 9</math>)</b> – species foraging on aquatic vegetation (including seeds) either below or above the water surface (algae, pondweed, waterside vegetation). The species collects vegetation while under water, sitting on the water surface or wading.
	<b>Aquatic surface (PAQSU, <math>n = 47</math>)</b> – species foraging on aquatic vegetation (including seeds) on/under water whilst swimming on the water surface. The species may dip under the water but, in contrast to PAQDI, contact with the surface is maintained.
	<b>Aquatic dive (PAQDI, <math>n = 13</math>)</b> – species foraging on aquatic vegetation (including seeds) under water by diving from the surface.
<b>Frugivore</b> ( $n = 1030$ )	<b>Aerial (FAE, <math>n = 88</math>)</b> – species foraging on fruits in flight, including those that hover to pluck fruit from bushes and trees (e.g. oilbird, some manakins).
	<b>Glean (FGL, <math>n = 894</math>)</b> – species foraging on fruits while perched (not in flight) above ground and plucking fruits from vegetation (e.g. toucans, hornbills).
	<b>Ground (FGR, <math>n = 20</math>)</b> – species foraging on fruits lying on the ground (e.g. trumpeters).

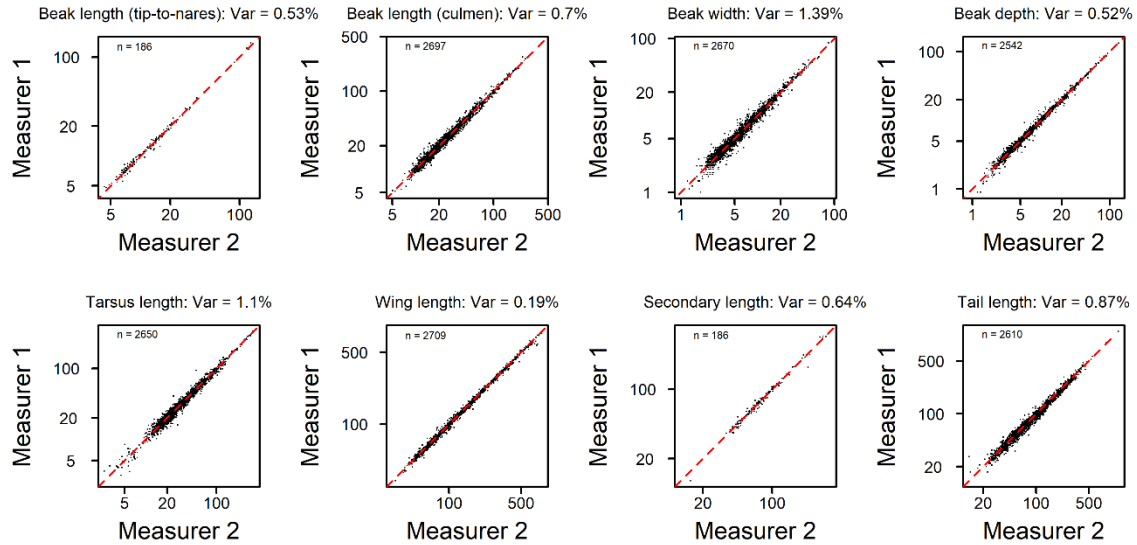
$n$  = number of species within each specialist trophic and foraging niche. The number of species within a trophic niche is generally greater than the sum of the constituent foraging niches because some species ( $n = 642$ ) use multiple foraging manoeuvres and substrates in relatively equal proportions and are classed as foraging generalists.

778  
779



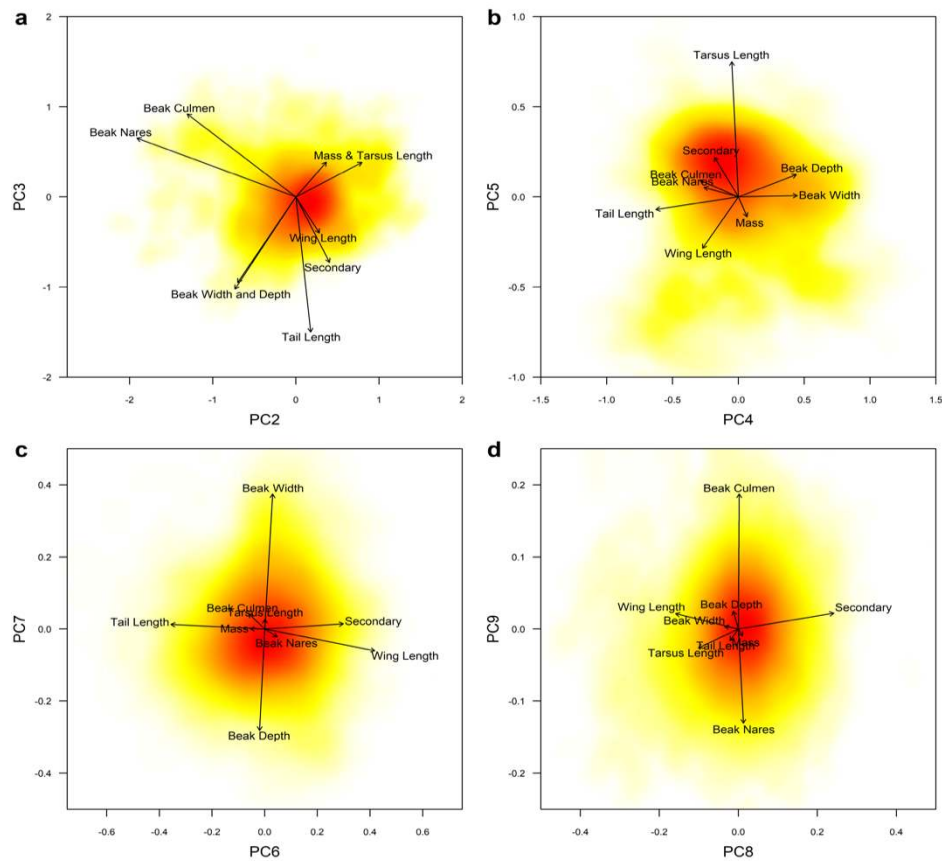
780  
781  
782  
783  
784  
785  
786  
787  
788  
789  
790  
791  
792  
793

**Extended Data Figure 1. Diagram of linear measurements of avian morphology.** **a**, Resident frugivorous tropical passerine (fiery-capped manakin, *Machaeropterus pyrocephalus*) showing four beak measurements: (1) beak length measured from tip to skull along the culmen; (2) beak length measured from the tip to the anterior edge of the nares; (3) beak depth; (4) beak width. **b**, Insectivorous migratory temperate-zone passerine (redwing, *Turdus iliacus*) showing five body measurements: (5) tarsus length; (6) wing length from carpal joint to wingtip; (7) secondary length from carpal joint to tip of the outermost secondary; (8) Kipp's distance, calculated as wing length minus first-secondary length; (9) tail length. Analyses exclude Kipp's distance, and thus include 8 traits shown here (plus body mass, making 9 traits in total). Illustration by Richard Johnson.

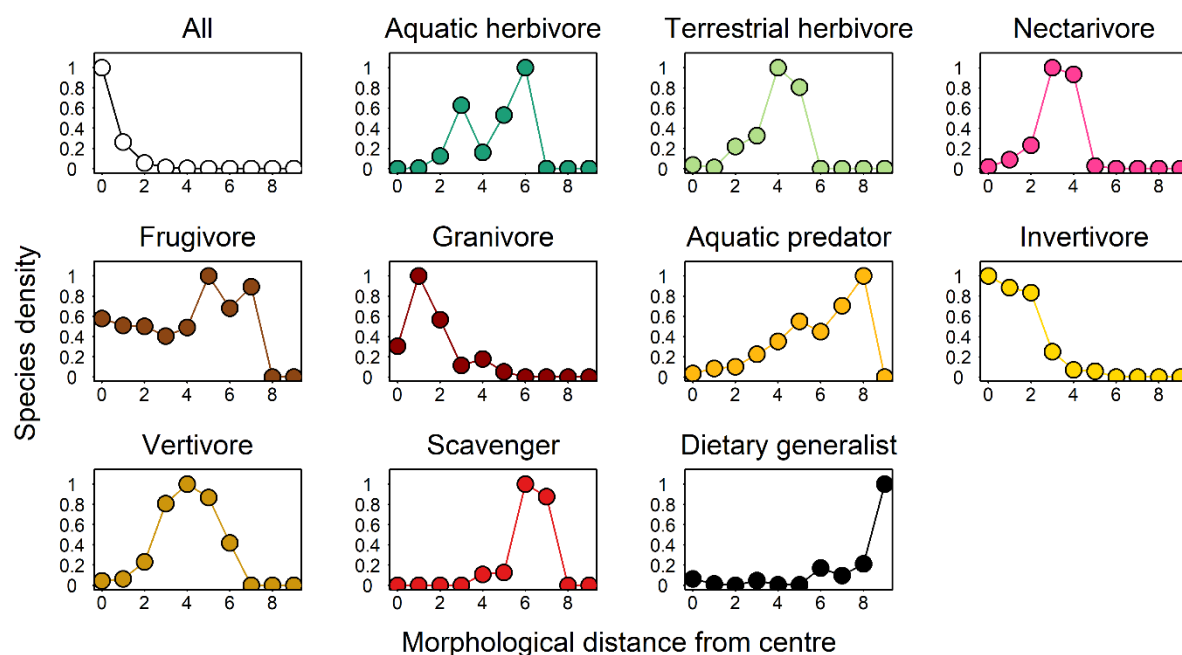


## Extended Data Figure 2. Repeatability of avian morphological trait

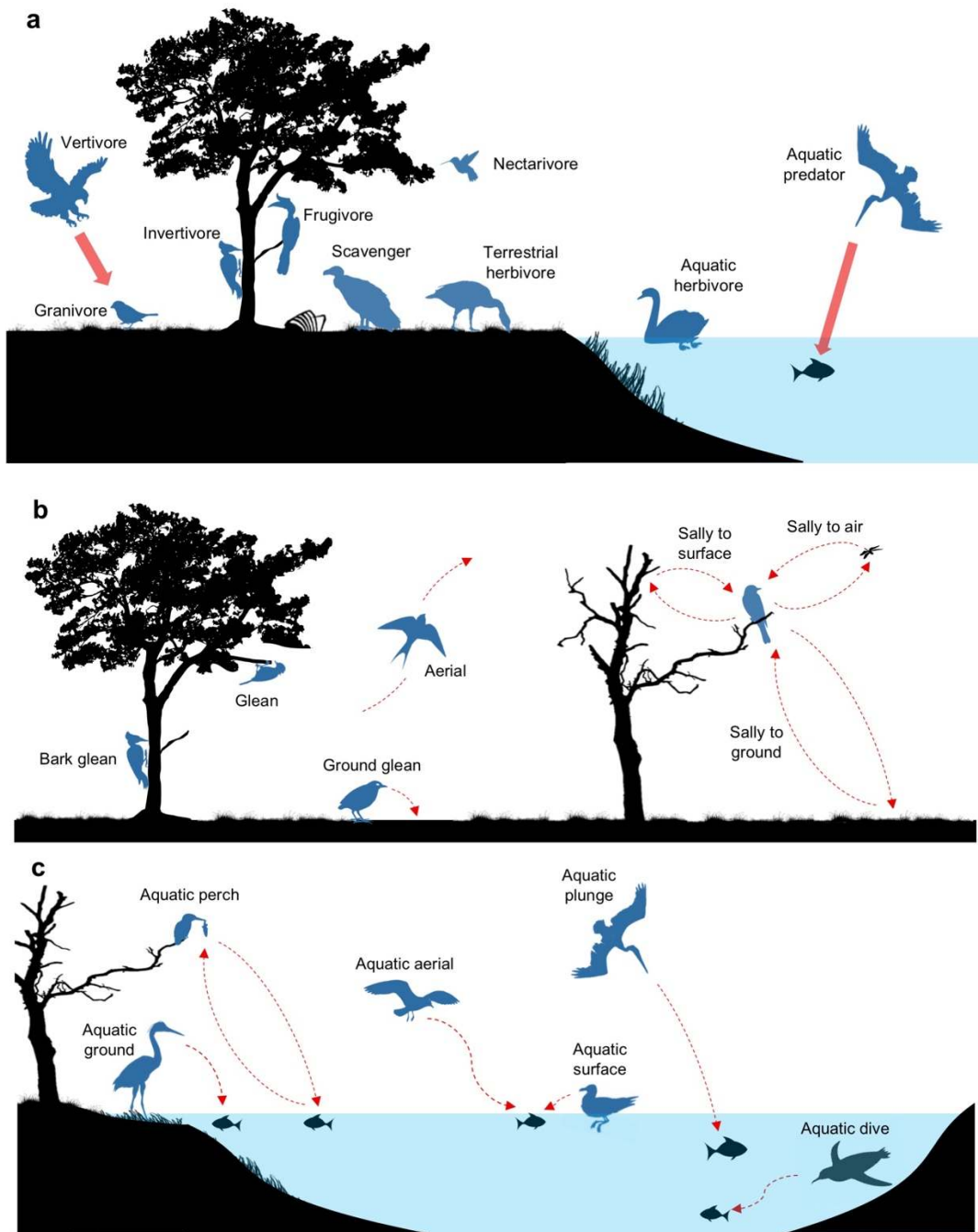
**measurements.** Data points show replicate measurements taken by different researchers on the same museum specimens for a subset of our global dataset ( $n = 2752$  specimens of  $n = 2523$  species). Points falling along the 1:1 line indicate a perfect correspondence between measurers. The % of total trait variance (Var) occurring between measurers within specimens is shown. The number of specimens varies across traits and is indicated in the top left of each plot.



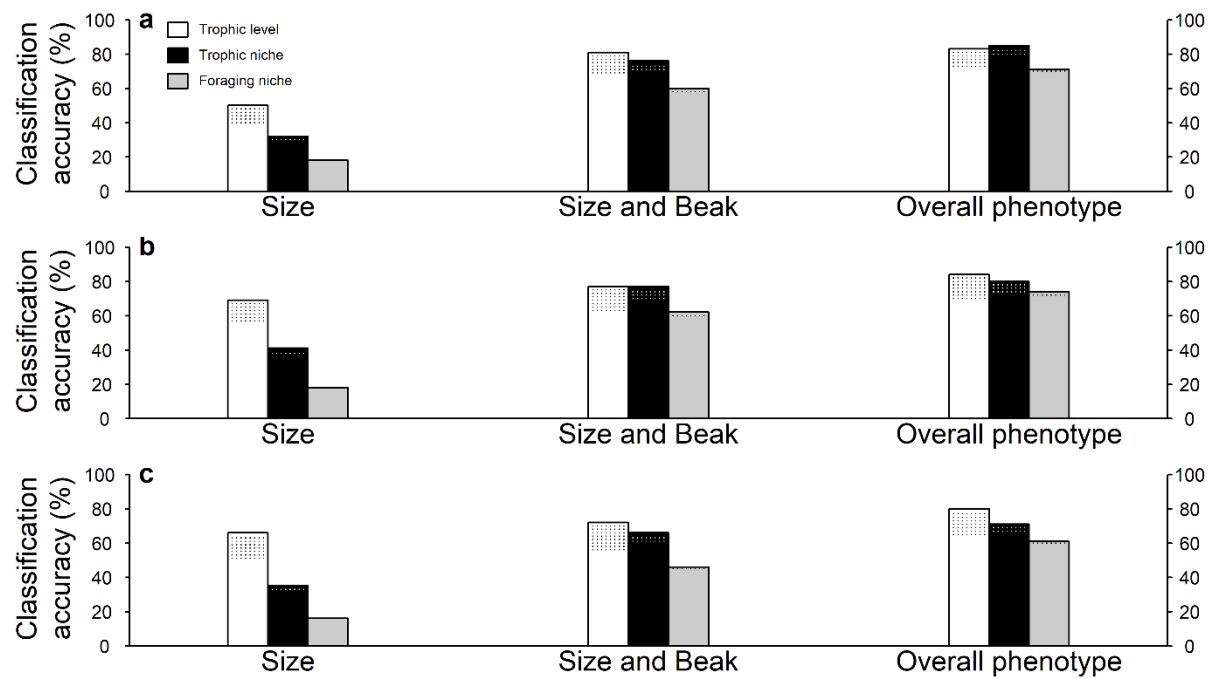
**Extended Data Figure 3. Trait loadings along principal component (PC) dimensions based on all 9 phenotypic traits.** Results are shown for PC axes representing variation in shape, and thereby excluding PC1 which represents variation in body size. Colours indicate the increasing density of species (from yellow to red) on each 2-dimensional plane (n = 9,963 species). See Extended Data Table 3 for trait loadings.



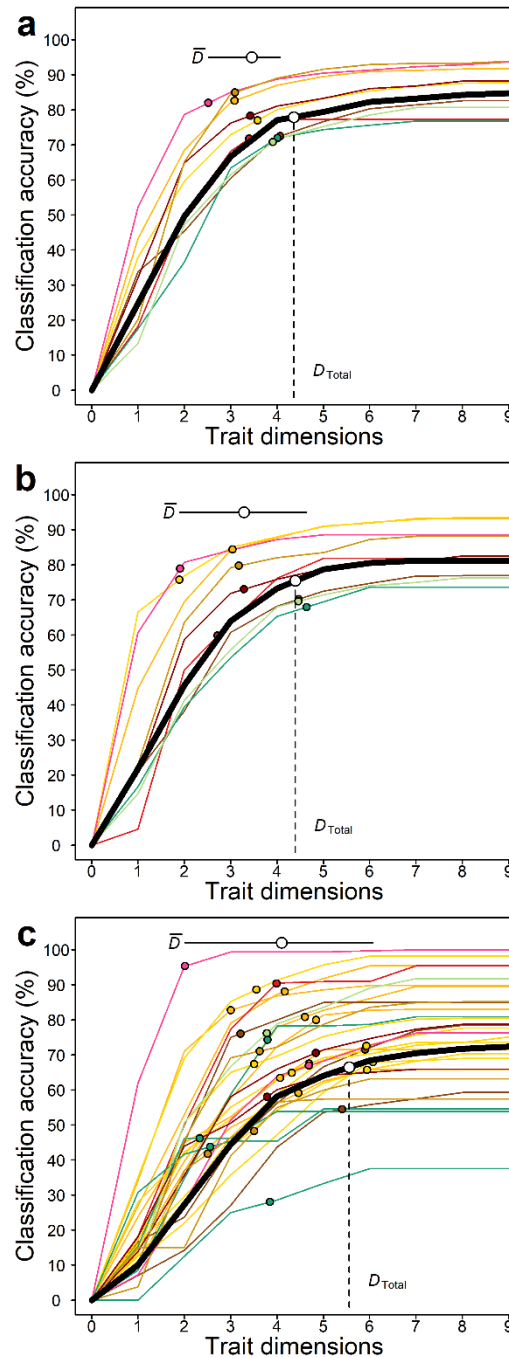
**Extended Data Figure 4. Density profiles through multidimensional morphospace.** The relative density of species with distance from the centroid of nine-dimensional morphospace is calculated for concentric shells of 1-unit diameter. Density is shown for all species ( $n = 9,963$ ) and each trophic niche separately.



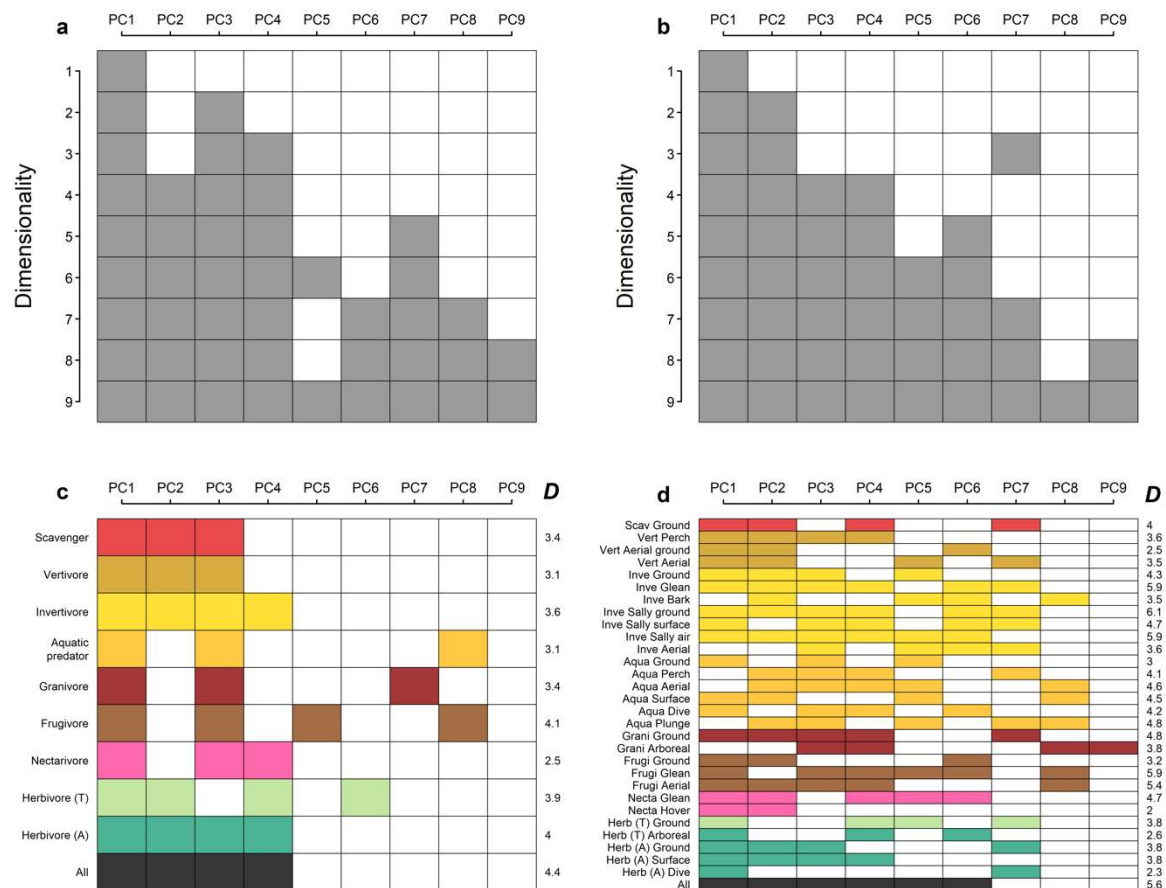
**Extended Data Figure 5. Avian trophic niches and foraging niches.** Silhouettes depict archetypal species belonging to (a) nine specialist trophic niches, (b) seven major foraging niches used by terrestrial invertivores, and (c) six major foraging niches used by aquatic predators. Foraging niches for the remaining seven specialist trophic niches are less diverse and are not shown. See Extended Data Table 4 for a full list and description of trophic and foraging niches.



**Extended Data Figure 6. Classification accuracy (%) using alternative classification algorithms.** Predictions of species trophic levels, trophic niches and foraging niches using (a) Random Forest, (b) Mixture Discriminant Analysis, and (c) Linear Discriminant Analysis for all birds ( $n = 9,963$  species) on the basis of body size (mass), size and beak traits, or the full nine-dimensional morphospace. Stippling indicates improvement in predictive accuracy after omitting omnivores and foraging generalists (see Methods).

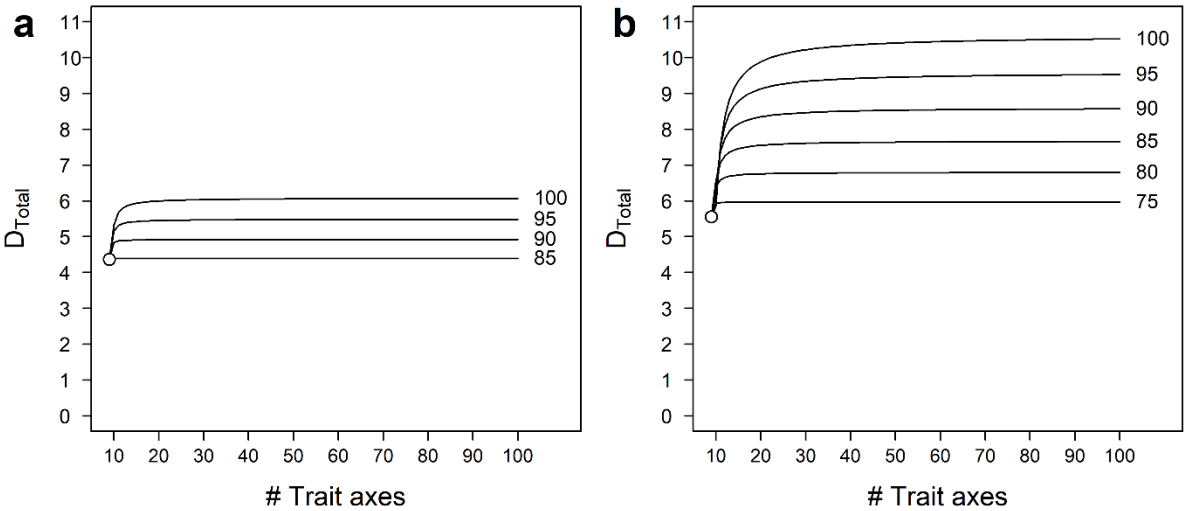


**Extended Data Figure 7. Intermediate dimensionality of avian niche space.** Accuracy curves indicate the maximum predictability of (a-b) trophic and (c) foraging niches in morphospaces consisting of different numbers of trait dimensions. Results are shown for a morphospace based on (a,c) standard and (b) phylogenetic principal components analysis. Accuracy is shown for individual niches (colours matching those depicted in Fig. 3) and total niche space (black,  $D_{Total}$ ). Points indicate the level of niche dimensionality ( $D$ ) according to Levene's index. Horizontal bar shows the mean ( $\bar{D}$ ) and range in dimensionality estimates for each niche.



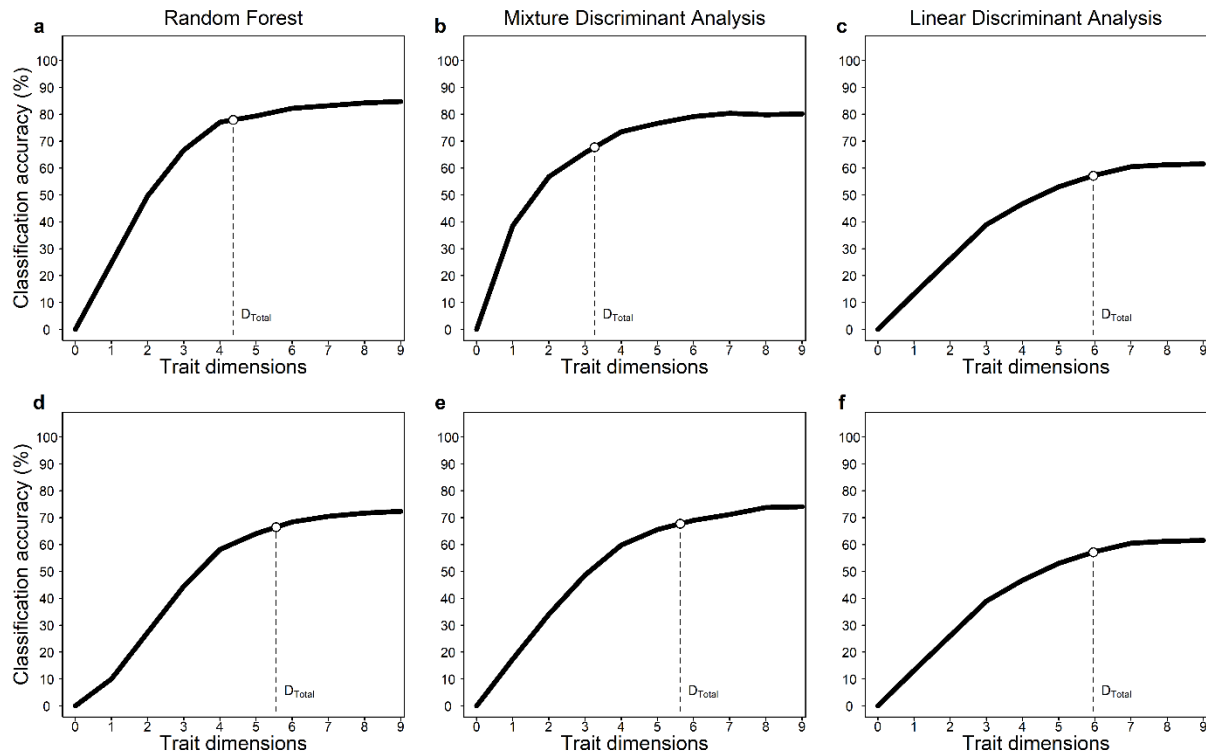
**Extended Data Figure 8. The dimensionality of avian trophic and foraging niches.** **a-b**, The identity of the trait dimensions best describing **(a)** trophic and **(b)** foraging niches for different levels of dimensionality. **c-d**, estimates of dimensionality (*D*) according to Levene's index for **(c)** trophic niches and **(d)** foraging niches. Each niche is given separately, and with all niches combined ('All'), along with the identity of the principal component (PC) dimensions (coloured squares) that best predict the niche.

873  
874



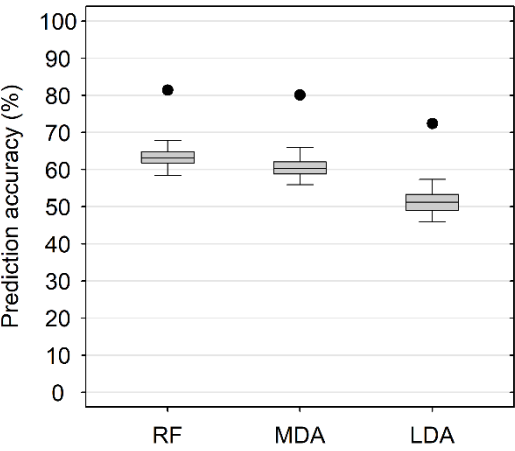
875  
876  
877  
878  
879  
880  
881  
882  
883  
884  
885  
886  
887  
888  
889  
890  
891  
892  
893

**Extended Data Figure 9. Estimated total dimensionality ( $D_{Total}$ ) of morphospace is robust to the inclusion of additional hypothetical trait axes.** Results are shown for (a) specialist trophic niches and (b) foraging niches. In addition to the nine measured traits, we simulated the effects of including additional hypothetical trait axes, up to a total of 100 axes. We assume that each additional trait axis has an equal contribution in accounting for the variation in niches currently unexplained by our empirical nine-dimensional morphospace. This assumption is conservative, because any variation in the relative contribution of these additional trait axes would lead to smaller increases in  $D_{Total}$  than estimated here. Thus, our simulations are best interpreted as providing an upper bound on  $D_{Total}$  from measuring additional trait axes.  $D_{Total}$  also depends on the assumption of whether these additional trait axes would enable ecological niches to be predicted with complete accuracy (i.e. 100%) or whether some variation in niches is inherently unpredictable. Assuming lower levels of maximum predictive accuracy (e.g. 85%) leads to less sensitivity in estimates of  $D_{Total}$  to variation in the number of trait axes.



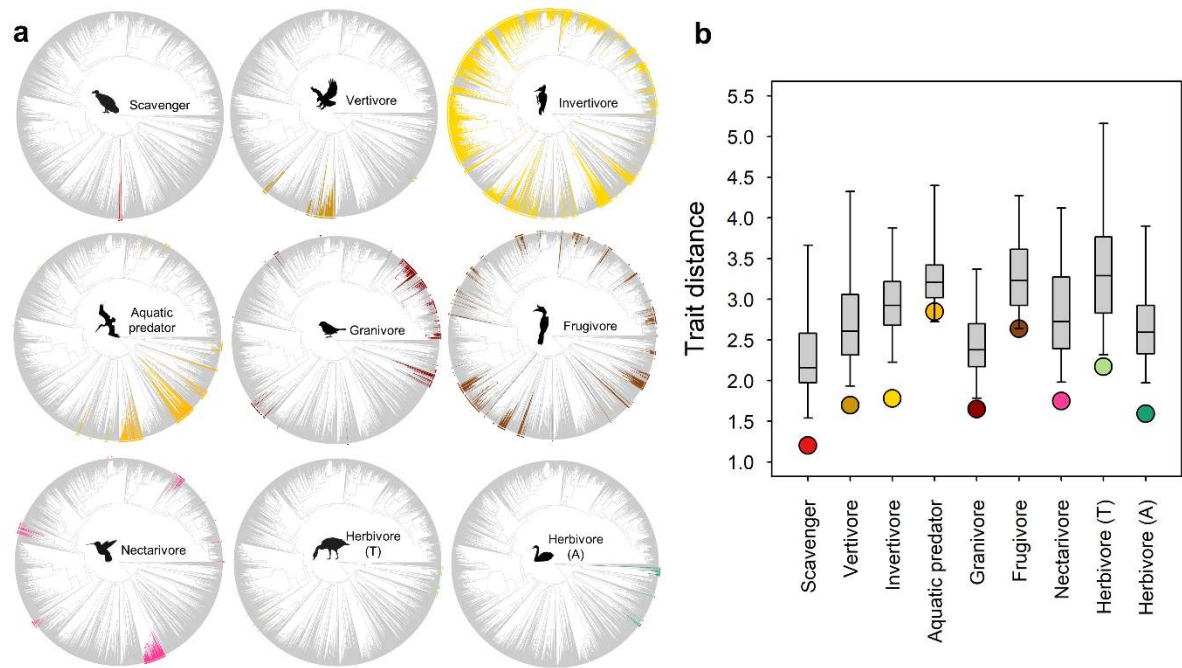
**Extended Data Figure 10. Estimating dimensionality of avian niche space using alternative classification algorithms** Random Forest (a,d), Mixture Discriminant Analysis (b,e) and Linear Discriminant Analysis (c,f). Accuracy curves indicate the cumulative maximum predictability of (a-c) trophic and (d-f) foraging niches in morphospaces consisting of different numbers of trait dimensions. Points indicate the dimensionality of niche space ( $D_{Total}$ ) according to Levene's index.

904  
905

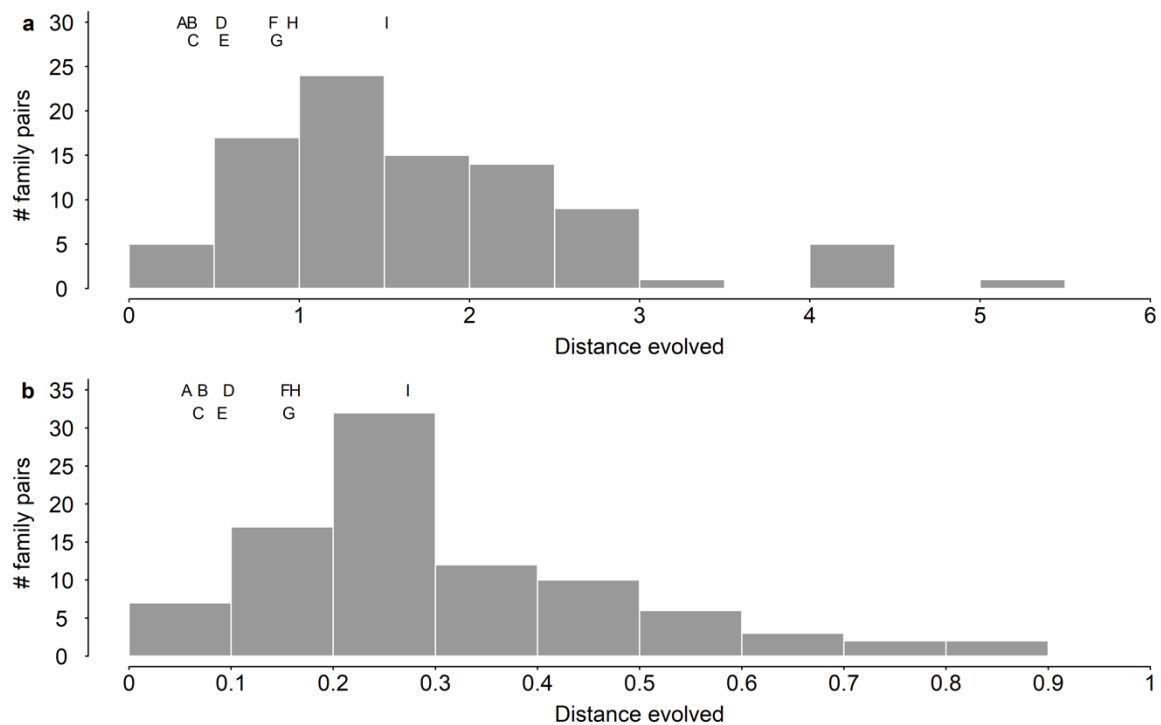


906  
907  
908  
909  
910  
911  
912  
913  
914  
915  
916  
917

**Extended Data Figure 11. The expected match between avian traits and trophic niches arising from shared phylogenetic history.** Boxplots show the predictive accuracy of three alternative classification algorithms— Random Forest (RF), Mixture Discriminant Analysis (MDA), and Linear Discriminant Analysis (LDA)—used to estimate trophic niches with the full nine-dimensional morphospace (points) for  $n = 6,666$  species with both morphological and genetic data. In each case, overall classification accuracy exceeds that expected under the evolutionary null model (box and whiskers show 50% interquartile range and 95% confidence interval). The null model incorporates a multi-rate process of Brownian trait evolution whereby rates of evolution can vary both across lineages and over time.



**Extended Data Figure 12. Non-random trait packing within avian trophic niches.** **a**, Phylogenetic distribution of avian trophic niches across the complete avian tree ( $n = 9,963$  species) with species lacking genetic data inserted according to taxonomic constraints<sup>41</sup>. Tips and internal branches connected by species sharing the same trophic niche are highlighted across the avian evolutionary tree. **b**, Mean pairwise trait distance between species in each trophic niche (points) is less than expected due to phylogenetic relatedness, based on species with both morphological and genetic data ( $n = 6,666$ ). Box and whiskers show 50% interquartile range and 95% confidence interval of mean pairwise trait distances expected under an evolutionary null model. This null model incorporates a multi-rate process of Brownian trait evolution whereby rates of evolution can vary both across lineages and over time.



**Extended Data Figure 13. The distance across morphospace independently evolved by phenotypically matched pairs of avian families.** We calculated the average phenotypic distance evolved by each clade since they last shared a common ancestor with their phenotypically matched family ( $n = 91$  pairs). Distances are expressed in (a) raw morphological units (trait axes scaled to unit variance) and (b) as a proportion of the total span of morphospace. On average, each clade within a matched family pair has independently evolved a distance equivalent to one-third of the total span of morphospace. For comparison, the 9 matched family pairs that are also sister clades (i.e. each other's closest relative) have each on average evolved a distance equivalent to only ~10% of the total span of morphospace. Position of letters indicate the average distance evolved by families within sister clades: (A) Cettiidae-Phylloscopidae, (B) Cardinalidae-Thraupidae, (C) Emberizidae-Passerellidae, (D) Phalacrocoracidae-Sulidae, (E) Odontophoridae-Phasianidae, (F) Strigidae-Tytonidae, (G) Ardeidae-Threskiornithidae, (H) Cacatuidae-Psittacidae, (I) Accipitridae-Cathartidae.

954     **References**

- 955     1     Elton, C. *Animal Ecology* (The Macmillan Company 1927).
- 956     2     Butterfield, N. J. Animals and the invention of the Phanerozoic Earth system. *Trends*  
957     *Ecol. Evol.* **26**, 81-87 (2011).
- 958     3     Estes, J. A. *et al.* Trophic downgrading of planet Earth. *Science* **333**, 301-306 (2011).
- 959     4     Dirzo, R. *et al.* Defaunation in the Anthropocene. *Science* **345**, 401-406 (2014).
- 960     5     Díaz, S. *et al.* The global spectrum of plant form and function *Nature* **529**, 167-171  
961     (2016).
- 962     6     Lauder, G. V. in *Functional Morphology in Vertebrate Paleontology* (ed J. J.  
963     Thomason) 1–18 (Cambridge University Press, 1995).
- 964     7     Carroll, S. Chance and necessity: the evolution of morphological complexity and  
965     diversity. *Nature* **409**, 1102-1109 (2001).
- 966     8     Wainwright, P. C. Functional versus morphological diversity in macroevolution.  
967     *Annu. Rev. Ecol. Evol. Syst.* **38**, 381-401 (2007).
- 968     9     Losos, J. B. Convergence, adaptation, and constraint. *Evolution* **65**, 1827-1840  
969     (2011).
- 970     10    Bascompte, J. & Jordano, P. Plant-animal mutualistic networks: the architecture of  
971     biodiversity. *Annu. Rev. Ecol. Evol. Syst.* **38**, 567-593 (2007).
- 972     11    Peck, A. L. *Aristotle: History of Animals*. (The Loeb Classical Library, 1970).
- 973     12    Cernansky, R. Biodiversity moves beyond counting species. *Nature* **546**, 22-24  
974     (2017).
- 975     13    Kraft, N. J. B., Godoy, O. & Levine, J. M. Plant functional traits and the  
976     multidimensional nature of species coexistence. *Proc. Natl. Acad. Sci. U.S.A.* **112**,  
977     797-802 (2015).
- 978     14    Larcombe, M. J., Jordan, G. J., Bryant, D. & Higgins, S. I. The dimensionality of  
979     niche space allows bounded and unbounded processes to jointly influence  
980     diversification. *Nat. Commun.* **9** (2018).
- 981     15    Diaz, S. & Cabido, M. Vive la difference: plant functional diversity matters to  
982     ecosystem processes. *Trends Ecol. Evol.* **16**, 646-655 (2001).
- 983     16    McGill, B. J., Enquist, B. J., Weiher, E. & Westoby, M. Rebuilding community  
984     ecology from functional traits. *Trends Ecol. Evol.* **21**, 178-185 (2006).
- 985     17    Lavorel, S. & Garnier, E. Predicting changes in community composition and  
986     ecosystem functioning from plant traits: revisiting the Holy Grail. *Funct. Ecol.* **16**,  
987     545-556 (2002).
- 988     18    Purves, D. *et al.* Time to model all life on Earth. *Nature* **493**, 295-297 (2013).
- 989     19    Didham, R. K., Leather, S. R. & Basset, Y. Circle the bandwagons – challenges  
990     mount against the theoretical foundations of applied functional trait and ecosystem  
991     service research. *Insect Conserv. Divers.* **9**, 1-3 (2016).
- 992     20    Gravel, D., Albouy, C. & Thuiller, W. The meaning of functional trait composition of  
993     food webs for ecosystem functioning. *Phil. Trans. R. Soc. B* **371** (2016).
- 994     21    Hutchinson, G. E. Concluding remarks. *Cold Spring Harbor Symposium Quantitative*  
995     *Biology* **22**, 415–427 (1957).
- 996     22    Schoener, T. W. Resource partitioning in ecological communities. *Science* **185**, 27-39  
997     (1974).
- 998     23    Cohen, J. E. *Food Webs and Niche Space* (Princeton University Press, 1978).
- 999     24    Williams, R. J. & Martinez, N. D. Simple rules yield complex food webs. *Nature* **404**,  
1000     180-183 (2000).
- 1001    25    Shoval, O. *et al.* Evolutionary trade-offs, pareto optimality, and the geometry of  
1002     phenotype space. *Science* **336**, 1157-1160 (2012).

- 1003 26 Blount, Z. D., Lenski, R. E. & Losos, J. B. Contingency and determinism in  
1004 evolution: replaying life's tape. *Science* **362** (2018).
- 1005 27 Winemiller, K. O., Fitzgerald, D. B., Bower, L. M. & Pianka, E. R. Functional traits,  
1006 convergent evolution, and periodic tables of niches. *Ecol. Lett.* **18**, 737-751 (2015).
- 1007 28 Laughlin, D. C. The intrinsic dimensionality of plant traits and its relevance to  
1008 community assembly. *J. Ecol.* **102**, 186-193 (2014).
- 1009 29 Petchey, O. L. & Gaston, K. J. Functional diversity (FD), species richness and  
1010 community composition. *Ecol. Lett.* **5**, 402-411 (2002).
- 1011 30 Eklof, A. *et al.* The dimensionality of ecological networks. *Ecol. Lett.* **16**, 577-583  
1012 (2013).
- 1013 31 Miles, D. B. & Ricklefs, R. E. The correlation between ecology and morphology in  
1014 deciduous forest passerine birds. *Ecology* **65**, 1629-1640 (1984).
- 1015 32 Pigot, A. L., Trisos, C. & Tobias, J. A. Functional traits reveal the expansion and  
1016 packing of ecological niche space underlying an elevational diversity gradient in  
1017 passerine birds. *Proc. Biol. Sci.* **283** (2016).
- 1018 33 Bright, J. A., Marugán-Lobón, J., Cobb, S. N. & Rayfield, E. J. The shapes of bird  
1019 beaks are highly controlled by nondietary factors. *Proc. Natl. Acad. Sci. U.S.A.* **113**,  
1020 5352–5357 (2016).
- 1021 34 Miller, E. T., Wagner, S. K., Harmon, L. J. & Ricklefs, R. E. Radiating despite a lack  
1022 of character: ecological divergence among closely related, morphologically similar  
1023 honeyeaters (Aves: Meliphagidae) co-occurring in arid Australian environments. *Am.*  
1024 *Nat.* **189**, E14-E30 (2017).
- 1025 35 Felice, R. N., Tobias, J. A., Pigot, A. L. & Goswami, A. Dietary niche and the  
1026 evolution of cranial morphology in birds. *Proc Biol Sci* **286**, 20182677 (2019).
- 1027 36 Navalón, G., Bright, J. A., Marugán-Lobón, J. & Rayfield, E. J. The evolutionary  
1028 relationship among beak shape, mechanical advantage, and feeding ecology in  
1029 modern birds. *Evolution* **73**, 422-435 (2019).
- 1030 37 Grinnell, J. The niche-relationships of the California Thrasher. *The Auk* **34**, 427–433  
1031 (1917).
- 1032 38 Bock, W. J. Concepts and methods in ecomorphology. *J. Biosciences* **19**, 403-413  
1033 (1994).
- 1034 39 Grant, P. R. *The ecology and evolution of Darwin's finches* (Princeton University  
1035 Press, 1999).
- 1036 40 Wilman, W., Belmaker, J., Simpson, J., de la Rosa, C. & Rivadeneira, M. M.  
1037 EltonTraits 1.0: Species-level foraging attributes of the world's birds and mammals.  
1038 *Ecology* **95**, 2027–2027 (2014).
- 1039 41 Jetz, W., Thomas, G. H., Joy, J. B., Hartmann, K. & Mooers, A. O. The global  
1040 diversity of birds in space and time. *Nature* **491**, 444-448 (2012).
- 1041 42 Ricklefs, R. E. & Travis, J. A morphological approach to the study of avian  
1042 community organization. *Auk* **97**, 321-338 (1980).
- 1043 43 Cooney, C. R. *et al.* Mega-evolutionary dynamics of the adaptive radiation of birds.  
1044 *Nature* **542**, 344-347 (2017).
- 1045 44 Peters, R. H. *The ecological implications of body size*. Vol. 2 (Cambridge University  
1046 Press, 1986).
- 1047 45 Sugihara, G. Minimal community structure: an explanation of species abundance  
1048 patterns. *Am. Nat.* **116**, 770-787 (1980).
- 1049 46 Harvey, P. H. & Pagel, M. *The comparative method in evolutionary biology*. (Oxford  
1050 University Press, 1991).
- 1051 47 Mahler, D. L., Ingram, T., Revell, L. J. & Losos, J. B. Exceptional convergence on the  
1052 macroevolutionary landscape in island lizard radiations. *Science* **341**, 292-295 (2013).

1053 48 Moen, D. S., Morlon, H. & Wiens, J. A. Testing convergence versus history:  
1054 Convergence dominates phenotypic evolution for over 150 million years in frogs. *Syst*  
1055 *Biol* **65**, 146-160 (2016).

1056 49 Muschick, M., Indermaur, A. & Salzburger, W. Convergent evolution within an  
1057 adaptive radiation of cichlid fishes *Curr. Biol.* **22**, 2362-2368 (2012).

1058 50 Mazel, F. *et al.* Prioritizing phylogenetic diversity captures functional diversity  
1059 unreliably. *Nat. Comm.* **9** (2018).

1060 51 Naeem, S., Duffy, J. E. & Zavaleta, E. The functions of biological diversity in an age  
1061 of extinction. *Science* **336**, 1401-1406 (2012).

1062 52 Sekercioglu, Ç. H., Wenny, D. G. & Whelan, C. J. *Why Birds Matter: Avian*  
1063 *Ecological Function and Ecosystem Services* (University of Chicago Press, Chicago,  
1064 2016).

1065 53 Derryberry, E. P. *et al.* Lineage diversification and morphological evolution in a  
1066 large-scale continental radiation: the Neotropical ovenbirds and woodcreepers (Aves:  
1067 Furnariidae). *Evolution* **65**, 2973–2986 (2011).

1068 54 Ricklefs, R. E. Passerine morphology: external measurements of approximately one-  
1069 quarter of passerine bird species. *Ecology* **98**, 1472 (2017).

1070 55 Dunning, J. B. *CRC Handbook of Avian Body Masses*. (CRC Press, 1993).

1071 56 Burin, G., Kissling, W. D., Guimarães, P. R. J., Şekercioğlu, Ç. H. & Quental, T. B.  
1072 Omnivory in birds is a macroevolutionary sink. *Nat. Comm.* **7**, 11250 (2016).

1073 57 del Hoyo, J., Elliott, A., Sargatal, J., Christie, D. A. & de Juana, E. *Handbook of the*  
1074 *Birds of the World* (Lynx Edicions, 2016).

1075 58 Remsen, J. V. & Robinson, S. K. A classification scheme for foraging behaviour of  
1076 birds in terrestrial habitats. *Stud. Avian Biol.* **13**, 144-160 (1990).

1077 59 Croxall, J. P. *Seabirds: feeding ecology and role in marine ecosystems* (Cambridge  
1078 University Press, 1987).

1079 60 Ashmole, N. P. in *Avian biology*. Vol. 1 (eds D. S. Farner & J. P. King) 223-286  
1080 (Academic Press, 1971).

1081 61 Fitzpatrick, J. W. Form, foraging behavior, and adaptive radiation in the Tyrannidae.  
1082 *Ornithol. Monogr.* **36**, 447-470 (1985).

1083 62 Hackett, S. J. *et al.* A phylogenomic study of birds reveals their evolutionary history.  
1084 *Science* **320**, 1763-1768 (2008).

1085 63 Drummond, A. J. & Rambaut, A. BEAST: Bayesian evolutionary analysis by  
1086 sampling trees. *BMC Evol. Biol.* **7**, 214 (2007).

1087 64 ArcGIS Desktop: Release 10.3 (Redlands, CA: Environmental Systems Research  
1088 Institute, 2014).

1089 65 Breiman, L. Random forests. *Machine Learning* **45**, 15–32 (2001).

1090 66 R: A language and environment for statistical computing (Vienna, Available at:  
1091 <http://cran.r-project.org/>. 2015).

1092 67 Liaw, A. & Wiener, M. Classification and Regression by randomForest. *R News* **2**,  
1093 18-22 (2002).

1094 68 Grundler, M. & Rabosky, D. L. Trophic divergence despite morphological  
1095 convergence in a continental radiation of snakes. *Proc. Biol. Sci.* **281** (2014).

1096 69 Rabosky, D. L. *et al.* BAMMtools: an R package for the analysis of evolutionary  
1097 dynamics on phylogenetic trees. *Methods Ecol. Evol.* **5**, 701-707 (2014).

1098 70 Rabosky, D. L. *et al.* Rates of speciation and morphological evolution are correlated  
1099 across the largest vertebrate radiation. *Nat. Commun.* **4**, 1958 (2013).

1100 71 Nosil, P. & Harmon, L. J. in *Speciation and patterns of diversity* (eds R. Butlin, J.  
1101 Bridle, & D. Schluter) 127-154 (Cambridge University Press, 2009).

1102 72 Rayner, J. M. V. in *Current Ornithology*. Vol. 5 (ed R. F. Johnston) 1-66 (Springer,  
1103 1988).

1104 73 Revell, L. J. Size-correction and principal components for interspecific comparative  
1105 studies. *Evolution* **63**, 3258-3268 (2009).

1106 74 Sidlauskas, B. Continuous and arrested morphological diversification in sister clades  
1107 of characiform fishes: a phylomorphospace approach. *Evolution* **62**, 3135-3156  
1108 (2008).

1109 75 Stayton, C. S. The definition, recognition, and interpretation of convergent evolution,  
1110 and two new measures for quantifying and assessing the significance of convergence.  
1111 *Evolution* **69**, 2140-2153 (2015).

1112 76 Holt, B. G. *et al.* An update of Wallace's zoogeographic regions of the world. *Science*  
1113 **339**, 74-78 (2013).  
1114

1115 **Acknowledgements:**

1116 We are grateful to numerous field biologists and explorers who collected and prepared  
1117 the specimens used in this study. We thank the Natural History Museum, Tring, UK, the  
1118 American Museum of Natural History, USA, and 63 other research collections for  
1119 providing access to specimens. Illustrations are reproduced with permission of Lynx  
1120 Edicions. Financial support was received from a Royal Society University Research  
1121 Fellowship (ALP); a PhD studentship funded by the Oxford Clarendon Fund and the US-  
1122 UK Fulbright Commission (CS); and Natural Environment Research Council grants  
1123 NE/I028068/1 and NE/P004512/1 (JAT). Secondary sources of funding are listed in  
1124 Supplementary Information, along with a complete list of individuals and institutions  
1125 that contributed directly to data collection, logistics and specimen access.

1126

1127 **Author Information**

1128

1129 **Affiliations**

1130 Centre for Biodiversity and Environment Research, Department of Genetics, Evolution  
1131 and Environment, University College London, Gower Street, London, WC1E 6BT, UK.

1132 Alex Pigot

1133 Department of Zoology, University of Oxford, South Parks Road, Oxford, OX1 3PS, UK.

1134 Tom P. Bregman, Alex Pigot, Catherine Sheard, Uri Roll, Nathalie Seddon, Joseph A.

1135 Tobias, Christopher H. Trisos

1136 School of Biology, University of St. Andrews, Fife, KY16 9TJ, UK.

1137 Catherine Sheard

1138 Cornell Lab of Ornithology, 159 Sapsucker Woods Rd., Ithaca, NY 14850, USA.

1139 Eliot T. Miller

1140 Department of Biological Sciences, University of Idaho, Moscow, Idaho 83844, USA.

1141 Eliot T. Miller

1142 Global Canopy Programme, 3 Frewin Chambers, Frewin Court, Oxford, OX1 3HZ, UK.

1143 Tom P. Bregman

1144 Biodiversity Research Centre, University of British Columbia, 6270 University Blvd.,

1145 Vancouver BC, V6T 1Z4, Canada.

1146 Benjamin G. Freeman

1147 Mitrani Department of Desert Ecology, Jacob Balaustein Institutes for Desert Research,

1148 Ben-Gurion University of the Negev, Midreshet Ben-Gurion 8499000, Israel.

1149 Uri Roll

1150 African Climate and Development Initiative, University of Cape Town, South Africa.

1151 Christopher H. Trisos

1152 Department of Life Sciences, Imperial College London, Silwood Park, Buckhurst Road,

1153 Ascot SL5 7PY, UK.

1154 Daniel Swindlehurst, Joseph A. Tobias

1155 Department of Ecology, Evolution and Environmental Biology, Columbia

1156 University, 1200 Amsterdam Avenue MC5557, New York, NY 10027, USA.

1157 Brian C. Weeks

Department of Ornithology, American Museum of Natural History, 79<sup>th</sup> Street at Central  
Park West, New York, NY 10024, USA.  
Brian C. Weeks

### **Contributions**

This study was conceived and coordinated by JAT and ALP, and designed by JAT, ALP, CS, ETM and UR. Morphological, ecological and geographic data were compiled by CS, ALP, TB, BF, UR, CT, DS, BW, NS and JAT. Analyses were led by ALP, and all authors contributed to writing the manuscript.

### **Competing interests**

The authors declare no competing financial interests.

### **Correspondence**

Correspondence and requests for information should be addressed to Alex Pigot ([a.pigot@ucl.ac.uk](mailto:a.pigot@ucl.ac.uk)) and Joseph Tobias ([j.tobias@imperial.ac.uk](mailto:j.tobias@imperial.ac.uk)) .

### **Reprints and permissions**

Reprints and permissions information is available at [www.nature.com/reprints](http://www.nature.com/reprints).